Functional Brain SPECT: The Emergence of A Powerful Clinical Method

B. Leonard Holman and Michael D. Devous, Sr.

Department of Radiology, Harvard Medical School and Brigham and Women's Hospital, Boston, Massachusetts and Department of Radiology, University of Texas Southwestern Medical Center, Dallas, Texas

J Nucl Med 1992; 33:1888–1904

Single-photon emission computed tomography (SPECT) techniques provide a powerful window into the function of the brain and promise to become an important component of the routine clinical evaluation of patients with neurological and psychiatric diseases. While it initially appeared that brain SPECT would suffer from a number of limitations relative to positron emission tomography (PET), recent improvements in instrumentation and radiopharmaceuticals as well as increasingly compelling clinical evaluations suggest a primary role for SPECT in the diagnosis of a number of highly prevalent neurological diseases. SPECT imaging, even with high-resolution systems, is substantially less expensive than PET and is more widely available. Furthermore, a number of novel approaches to diagnosis have been developed for SPECT exclusively. The implementation of this method into clinical practice has been slow, however, and its appropriate utilization will require much closer collaboration between nuclear medicine physicians, neurologists, psychiatrists and neurosurgeons.

RADIOPHARMACEUTICALS

Functional brain imaging requires radiotracers that cross the blood-brain barrier, distribute proportionally to regional cerebral blood flow and remain fixed in the brain for a sufficiently long time to permit SPECT imaging. Alternatively, blood flow can be measured quantitatively from the clearance of the inert gas ^{133}Xe with highly sensitive instrumentation that can image its distribution repeatedly during its rapid clearance from the brain.

For radiotracers that have a very slow clearance from the brain, estimates of regional cerebral blood flow (rCBF) are based on the microsphere model, which assumes that the radiotracer is freely diffusible from the blood pool, that it is completely extracted from the blood into the brain and that it remains fixed within the brain without redistribution. Of course, only microspheres injected directly into the carotid artery satisfy these requirements completely. Nevertheless, those radiotracers that are available for brain perfusion imaging follow rCBF closely enough to be clinically useful. Furthermore, most routine clinical applications of brain perfusion SPECT do not require quantitation of rCBF and rely on the generation of images which reflect tracer uptake and retention only. Quantitation of regional cerebral blood flow with these radiotracers requires arterial sampling and careful modeling to account for incomplete extraction, back flux from the brain and other deviations from the theoretical model (*1*). Despite these constraints, intravenous injection of brain perfusion radiotracers results in regional brain activity which correlates well with independent measures of rCBF over a wide range of flows.

Iodine-123-isopropyl iodoamphetamine (IMP, Spectamine) was the first brain perfusion tracer to be synthesized and remains the most ideal with respect to its kinetics (*2,3*). Iodine-123 is not an ideal radionuclide since it is not generator-produced and emits high-energy photons. The distribution of IMP reflects rCBF over a wide range of flows but may underestimate flow when plasma pH is low, as in cerebral ischemia or acidosis (*1*). Its first-pass extraction by the brain is high, and peak activity is reached within 15 to 20 min (*4*). Brain imaging must be accomplished quickly after injection since redistribution is fairly rapid and significant changes can be observed after 60 min. Since [^{123}I]IMP is prelabeled by the commercial supplier, logistic problems occur and emergency studies are difficult to schedule. With the standard injected dose of 3–6 mCi, the photon flux is low and image quality is not as good as that with the technetium-labeled ligands. This becomes a particular problem with high-resolution imaging systems.

Technetium-99m brain perfusion agents benefit from the optimal physical characteristics of the radionuclide, including its 140 keV monoenergetic photon, 6-hr half-life and potential for on-site labeling. Of the ^{99m}Tc radiopharmaceuticals that have been synthesized, only ^{99m}Tc-HMPAO (hexamethylpropyleneamine oxime, Ceretec) is currently available in the United States. It is a highly

Received Apr. 15, 1992; revision accepted Jun. 4, 1992.
For reprints contact: B. Leonard Holman, MD, Chairman, Department of Radiology, Brigham and Women's Hospital, 75 Francis St., Boston, MA 02115.

soluble macrocyclic amine with rapid brain uptake but only moderate first-pass extraction, which results in underestimation of rCBF (*5,6*). When regional cerebral blood flow is quantified, this underestimation can be corrected by accounting for the freely exchangeable component of HMPAO. Of the brain perfusion agents, ^{99m}Tc-HMPAO is the closest to a microsphere with virtually no brain washout. The tracer remains fixed in the brain following conversion to a hydrophilic compound in the presence of intercellular glutathione (*7*). Because blood clearance is slow, perfusion defects are not seen as sharply as with other brain perfusion tracers. Technetium-99m-HMPAO follows blood flow and, when flow and metabolism are uncoupled as they are in luxury perfusion, ^{99m}Tc-HMPAO may be increased or normal, while [^{123}I]IMP may indicate a profound metabolic defect (*8*). The radiopharmaceutical is chemically unstable in vitro and must be injected immediately after preparation.

Technetium-99m-ECD (ethyl cysteinate dimer, Neurolite) is currently undergoing clinical testing (*9,10*). Like ^{99m}Tc-HMPAO, it has moderate cerebral extraction and underestimates rCBF. Brain uptake is rapid and clearance from the brain is very slow. Blood clearance is rapid, resulting in a higher brain-to-background activity ratio than with HMPAO. Furthermore, ^{99m}Tc-ECD is stable in vitro.

With the inert gas clearance technique, rCBF is estimated from the clearance of ^{133}Xe from the brain following inhalation of the gas (*11,12*). This methodology can be coupled with SPECT with specially designed instrumentation. Because of the rapid clearance of the tracer, multiple studies can be performed on the same day. Quantitative measures can be obtained without arterial sampling. Limitations of ^{133}Xe SPECT include the low photon energy of the tracer and its rapid clearance from the brain, which lead to poor spatial resolution. Specialized instrumentation is required with very high sensitivity in order to obtain multiple images during the clearance of the tracer from the brain. The inhalation technique is more technically difficult than the intravenous method using brain perfusion radiotracers.

INSTRUMENTATION

A wide variety of imaging systems capable of high-resolution brain SPECT are now available commercially. They fall into two categories: noncamera-based and camera-based systems. Noncamera-based systems include rotating detector arrays, fixed detector systems and multidetector scanners. The rotating detector array group includes the Hitachi four-head system, and the more prevalent Tomomatic two-, three- and five-slice machines (Medimatic, Inc). The Tomomatic's most characteristic attribute is that it is capable of ^{133}Xe SPECT, because it has high sensitivity and can do rapid dynamic imaging (*12*). The Tomomatic, by changing collimators, can also produce images of relatively high resolution (9–10 mm) using ^{99m}Tc-HMPAO or [^{123}I]IMP. Collimator exchange is not difficult, permitting case-by-case selection between ^{133}Xe and high-resolution scans. The Hitachi rotating detector array system is also capable of both ^{133}Xe and high resolution (8–10 mm) static imaging (*13*).

The original fixed-detector research systems that use multiple detectors were the SPRINT (*14*) and the HEADTOME (*15*). They were designed with fixed detectors oriented in a ring geometry with an internally rotating collimator. The Shimadzu (HEADTOME) system, which is commercially available, is capable of high sensitivity ^{133}Xe studies and moderate spatial resolution (10–12 mm) using ^{123}I or ^{99m}Tc.

The original multidetector scanner was the unit developed by Stoddart and colleagues (*16*), also known as the Harvard multidetector scanner (*17*), and is commercially available as the Strichman unit. This is a slice-based tomograph, as are the Hitachi, Shimadzu and Tomomatic, but it is built with very thick crystals that operate much like pinhole cameras as they traverse through space to obtain tomographic data. Hill et al. have demonstrated that this device can image not only ^{99m}Tc and ^{123}I, but also ^{18}F in a single-photon (not PET) mode (*18*). It cannot perform ^{133}Xe SPECT.

Gamma camera-based systems are more prevalent today than dedicated tomographs, primarily because they can do both head and body SPECT. There are two forms: single-head and multihead systems. Modern tomographs have overcome many of the limitations of the original systems, such as poor head alignment, magnetic field aberrations and inadequate uniformity and linearity for tomography. A few of the modern single-head systems have also been designed to circumvent shoulders so that minimal radius scanning is possible. Most of these systems provide fairly high-resolution images with static tracers. Unfortunately, they suffer from poor sensitivity and prolonged imaging times.

Researchers from the University of Texas Southwestern Medical Center at Dallas, in collaboration with the nuclear engineering division of Technicare, developed the first three-head gamma camera SPECT system (*19*) to address the limited sensitivity of single-head systems. Their intent was to provide a system capable of both body and head SPECT at high resolution with static tracers and with adequate sensitivity and rotation speed for dynamic tomography with ^{133}Xe. The first three-head system was installed in Dallas in late 1987 under the sponsorship of Ohio Imaging, now a division of Picker. Additional three-head SPECT instruments have been produced by Trionix and Toshiba. Prototype three-head instruments from General Electric and Siemens are also under evaluation. Currently, there are approximately 150 such units installed, indicating increasing acceptance of this technology.

A variant of the gamma camera approach utilizes a single annular sodium iodide crystal (*20–22*). The ASPECT system, which is now commercially available, uses

a fixed annulus with rotating collimators (*22*). It yields high spatial resolution (5.5–6.5 mm) with excellent sensitivity. Xenon-133 dynamic SPECT acquisition is currently under development.

State-of-the-art SPECT systems can be expected to provide high-resolution (6–9 mm) imaging of statically distributed brain radiopharmaceuticals with patient imaging times of 10–20 min. All of the currently available three-head, annular and fixed detector ring systems (Picker, Trionix and Toshiba) offer excellent spatial resolution: with appropriate collimators and ^{99m}Tc-HMPAO, 6 mm resolution in the cortex and about 7 mm at the center of the brain. With [^{123}I]IMP, the photon flux is reduced, thus requiring careful image processing to achieve equivalent spatial resolution. Images of ^{99m}Tc-HMPAO and [^{123}I]IMP from the same normal control subject obtained on a three-headed tomograph are shown in (Fig. 1).

Systems should also be capable of sequential image acquisition; it should be possible to acquire multiple short studies back to back and subsequently discard segments degraded by patient motion. Software should support dynamic filtering, multiple angle (oblique) reconstructions, surface-variable attenuation correction and three-dimensional as well as conventional cross-sectional displays. The merging of anatomic information from CT and MRI with SPECT is also necessary for accurate diagnosis and localization (*23*) and should be a critical element of the software package. Three-head and annular systems in theory should be capable of ^{133}Xe SPECT. However, dynamic scanning has not been accomplished with any camera-based system. There is work in progress demonstrating such feasibility for the Picker and Toshiba systems.

SPECT systems should have adequate energy resolution and multiwindow capability in order to separate ^{99m}Tc and ^{123}I radiotracers in the same patient (*24,25*). While typical gamma-camera energy resolution (12%–15% FWHM) is insufficient to separate 140 keV (^{99m}Tc) from 159 keV (^{123}I) photopeaks, high-resolution multidetector SPECT units have substantially improved energy resolution. The images shown in Figure 1 were obtained simultaneously using dual-isotope imaging of ^{99m}Tc-HMPAO and [^{123}I] IMP.

CEREBROVASCULAR DISEASE

The measurement of rCBF in patients with cerebrovascular disease was the earliest application of SPECT of the brain. Numerous reports in the last decade describe applications for SPECT rCBF imaging in stroke, transient ischemic attacks (TIA), subarachnoid hemorrhage (SAH), arteriovenous malformation (AVM) and other derangements of cerebral hemodynamics. Several valuable reviews are available (*26–28*). Many of these reports promote both diagnostic and prognostic roles for SPECT rCBF imaging of cerebrovascular disease, although criticisms have been raised that current investigations do not directly address the questions of greatest importance to the referring physician (*29,30*).

SPECT is superior to anatomical imaging procedures in detecting cerebral ischemia during the first hours following an ictus because rCBF alterations occur earlier and are better defined than structural changes. Knowledge of perfusion status has important clinical applications in the differential diagnosis and initial management of patients

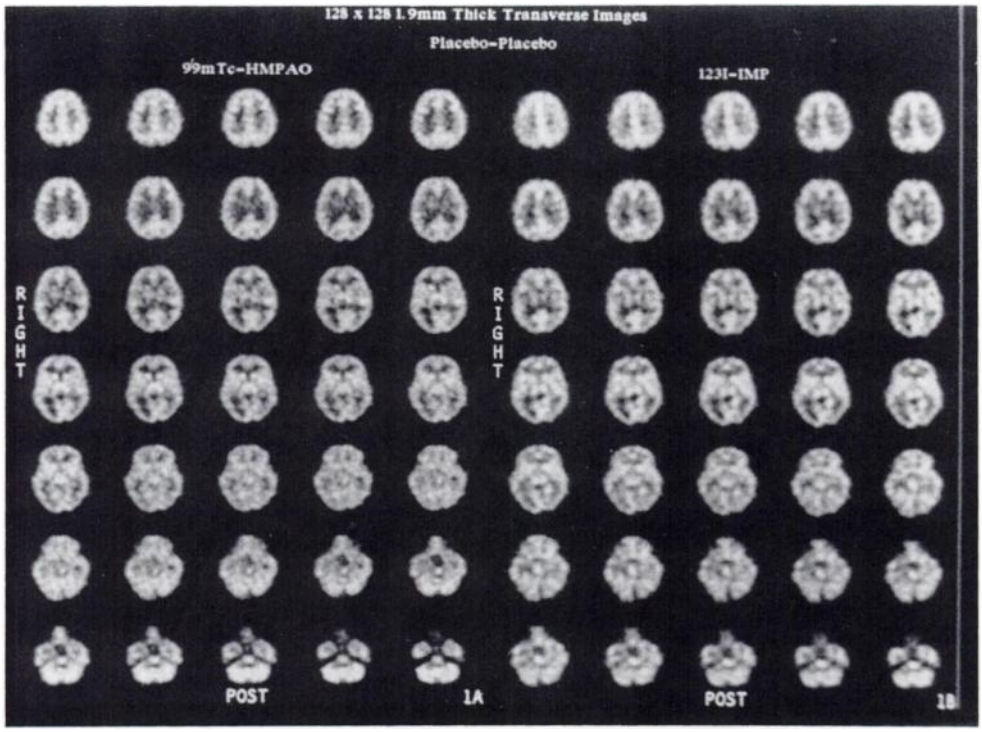

FIGURE 1. High-resolution SPECT images of ^{99m}Tc-HMPAO (left) and [^{123}I]IMP (right) in the same normal volunteer. Images were obtained simultaneously by dual-isotope acquisition of the two radiotracers injected sequentially. A 128 × 128 acquisition matrix was employed using a high-resolution (7–8 mm) fan beam collimator and a three-headed SPECT system. Note similar image resolution for both brain blood flow tracers.

with cerebrovascular disease. In patients with TIA, SPECT may provide the only objective documentation of the ictus. The detection of hemodynamic alterations is also important in patients with silent strokes and other asymptomatic lesions to facilitate patient subtyping and management.

Stroke

SPECT is useful in the detection of acute cerebral ischemia. Regional CBF alterations occur instantly in patients with stroke, while CT and MRI are typically normal during the first hours to days after the ictus (Fig. 2). For example, by 8 hr after infarction, only 20% of CT scans will be positive (*31,32*), while at the same time approximately 90% of SPECT rCBF scans will be abnormal (*33,34*). The difference in sensitivity between structural and functional imaging modalities disappears within about 72 hr. In addition, the sensitivity of SPECT is significantly reduced for lacunar infarctions.

Sensitivity for lesion detection is also affected by luxury perfusion (*35*), wherein perfusion and metabolism become decoupled beginning approximately 5 days after the ictus, and continuing for as much as 20 days (Fig. 3). Although this phenomenon is not well understood, it is well documented (*8,12,26,27*) and false-negative studies can result during this period. Thus, acute rCBF imaging may be effective, but imaging during the subacute phase is insensitive, particularly with ^{99m}Tc-HMPAO (*8*).

Crossed-cerebellar diaschisis frequently accompanies cortical strokes because cortico-pontine-cerebellar linkages normally provide stimulation to the cerebellum contralateral to the indicated cortex. Reduced perfusion to the contralateral cerebellum is a common secondary phenomenon following cerebral ischemia, which continues even during luxury perfusion (*36,37*).

SPECT rCBF imaging may also be useful in delineation of stroke subtypes. Since evolving therapeutic regimens are subtype-specific, it is increasingly important to provide rapid, accurate classification of the acute episodes. For example, case selection for endarterectomy may depend on the identification of patients with ongoing low-flow states even in the presence of asymptomatic carotid disease

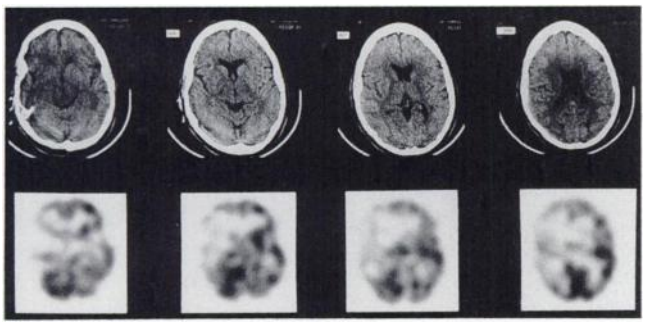

FIGURE 2. Abnormal perfusion in the distribution of the right middle cerebral artery in an acute stroke patient 6 hr after onset of symptoms. A concurrent CT scan was normal. A repeat CT study was abnormal three days after ictus.

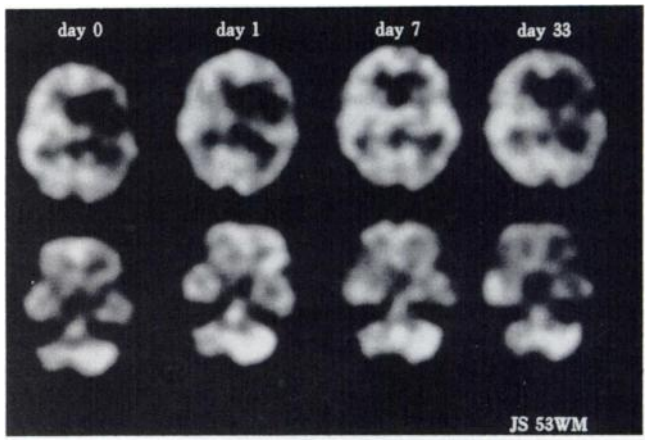

FIGURE 3. Mid-level and inferior level (containing cerebellum) SPECT brain blood flow images in a stroke subject demonstrate a left hemispheric flow deficit on the day of the ictus that partially resolves by 24 hr. Apparent resolution of the deficit at Day 7 represents luxury perfusion to an infarcted and metabolically abnormal zone. By Day 33, the flow disturbance returns to a level similar to that seen initially. Note that crossed cerebellar diaschisis is present and does not resolve during luxury perfusion.

(*28,30*). In acute infarctions, distinguishing between the appropriateness of anticoagulation or thrombolytic therapy may depend on the demonstration of the physiologic significance of an angiographically demonstrable lesion. The use of calcium channel blockers may only be effective prior to induced or spontaneous reperfusion.

The measurement of cerebrovascular reserve is particularly well suited to rCBF imaging. Two indices of reserve can be obtained. The rCBF-to-rCBV (flow/volume) ratio may be related to the regional oxygen extraction ratio and provides an indirect measure of perfusion pressure (*38–40*). Cerebrovascular reserve can also be measured following the vasodilatory response to CO_2, or acetazolamide, a carbonic anhydrase inhibitor and potent cerebral vasodilator (*41–43*). Measurements of cerebrovascular reserve are useful in assessing either the need for acute interventions following stroke or the risk status for secondary strokes. A recently developed dual-isotope imaging technique (*24*) facilitates the measurement of cerebrovascular reserve by SPECT (*25*) (Fig. 4).

Several recent studies also suggest a prognostic role for SPECT in stroke. A direct relationship between rCBF and clinical outcome has both been supported (*44–48*) and refuted (*49–51*). Improved correlation between rCBF and outcome has been achieved with measurement of the volume of the rCBF defect relative to the volume of structural defect (*52*) or of the volume of the flow lesion alone (*28,53–55*). One of these studies (*55*) showed a 92% predictive power of rCBF SPECT obtained within 6 hr of the ictus for poor neurologic outcome.

Distinctions between [^{123}I]IMP and ^{99m}Tc-HMPAO have been reported. IMP may provide more contrast for areas of ischemia than HMPAO, particularly in the subacute phase (*8,56*). Reduced lesion contrast with HMPAO

may be a consequence of flow-dependent backdiffusion (*57*) and high initial blood levels (*58*). A comparison of early and delayed (4 hr postinjection) IMP uptake has been proposed as an indicator of tissue viability (*47*), although this is not well established (*54*).

Transient Ischemic Attacks

Determination of the cause of a TIA (thrombotic, embolic or hemodynamic) has substantial impact on patient management. Structural imaging contributes little. For example, Crow and Guinto found that 82/100 TIA patients had normal CT scans; the 12 patients with abnormal scans showed only the nonspecific finding of atrophy (*59*). SPECT rCBF imaging may clarify the mechanism of ischemia (*60*) and may identify patients at the highest risk for subsequent infarction in the first week following TIA (*61*). The value of SPECT imaging in TIA patients may be increased by assessing the status of vasodilatory reserve and the response to medical or surgical intervention. Such assessments are important since as many as 60% of TIA patients will go on to have a completed stroke (*62*). The sensitivity of rCBF imaging in TIA declines with time, from 60% in the first 24 hr (*63*) to less than 40% 1 wk after the event (*34*). This sensitivity may be enhanced both early and late after the ischemic event by examination of cerebrovascular reserve with acetazolamide (*61,64*).

Subarachnoid Hemorrhage

Subarachnoid hemorrhage accounts for approximately one-half of all intracranial hemorrhagic strokes. Post-hemorrhage neurologic deficits that appear within 2 wk are most commonly a consequence of vasospasm (*65*). Consequent delayed cerebral ischemia and possible infarction make vasospasm an equally important factor with recurrent hemorrhage in the morbidity or mortality of subarachnoid hemorrhage. Management of subarachnoid hemorrhage patients requires the differentiation of vasospasm from edema, elevated intracranial pressure, hydrocephalus and electrolyte aberrations (*66*). Vasospasm is accompanied by decreased rCBF, decreased cerebral metabolism, increased neurologic deficit and increased cerebral blood volume (*67,68*). Davis et al. found a correlation between regional hypoperfusion evidenced by HMPAO SPECT and the presence and severity of a delayed neurologic deficit in subarachnoid hemorrhage patients (*69*). While the presence of vasospasm can be documented by transcranial Doppler (*70*) or angiography, these studies only indirectly relate to the risk for cerebral infarction. Regional CBF or rCBF/rCBV imaging provide a more direct measure of the hemodynamic significance of observed vasospasm. By providing early evidence of cerebral ischemia, SPECT may help to differentiate vasospasm from other causes of neurologic deterioration following subarachnoid hemorrhage and thus enhance delivery of therapeutic measures designed to reduce its effects.

Arteriovenous Malformation

Patients with arteriovenous malformation are at risk for three major complications: (1) intracerebral or intraventricular bleeding, which may occur at any time and may be fatal [the incidence of spontaneous hemorrhage ranges from 35% to 60% (*71*)]; (2) seizures; and (3) intracerebral "steal," in which relative ischemia is produced in parts of the brain either adjacent to or remote from the arteriovenous malformation due to high arterial-to-venous shunting through the arteriovenous malformation (*72*). Xenon-133 SPECT studies have demonstrated a high incidence of steal (*72–75*). Documentation of steal has provided a motivation for staging of surgical resection and for presurgical treatment with arterial embolization (*74,75*). The arteriovenous malformation itself appears as a high-flow region on ^{133}Xe SPECT, but as an area of reduced tracer uptake with IMP or HMPAO since the vascular malformation does not retain these tracers. Devous, Batjer and colleagues found that the examination of cerebrovascular reserve with acetazolamide in arteriovenous malformation patients was prognostic for postoperative outcome (*76, 77*).

Future Prospects

Even though SPECT rCBF measures provide sensitive early detection of cerebral ischemia, and may provide both diagnostic and prognostic information in stroke patients, no significant change in the frequency of referral from neurologists for SPECT has been observed. Brass and Ratner have identified several relevant factors (*30*). First, the complete implementation of rCBF SPECT imaging in the evaluation of patients with cerebrovascular disease will require a far more thorough interdigitization of the nuclear medicine physician and the neurologist in evaluating, improving and implementing this potentially valuable technique. Second, purely descriptive studies, often performed in isolation from a clear statement of relevant clinical problems, contribute little to understanding the role of SPECT rCBF measurements in patient management or enhancing the referring physician's perception of the usefulness of this technique. Prospective studies should be designed to answer focused questions relating to issues of clinical management. Finally, thorough evaluation of "brain stress tests," specifically the measurement of vasodilatory reserve, is important since current clinical or structural imaging measures are limited in their ability to determine risk status. An increased recognition of the importance of hemodynamic measures relative to structural assessments (*78*) places new emphasis on the evolution of activation or intervention studies (*42*) which enhance risk assessment. The current role for rCBF SPECT imaging in cerebrovascular disease can only be recognized and expanded through careful cooperative efforts between the nuclear medicine and neurological communities.

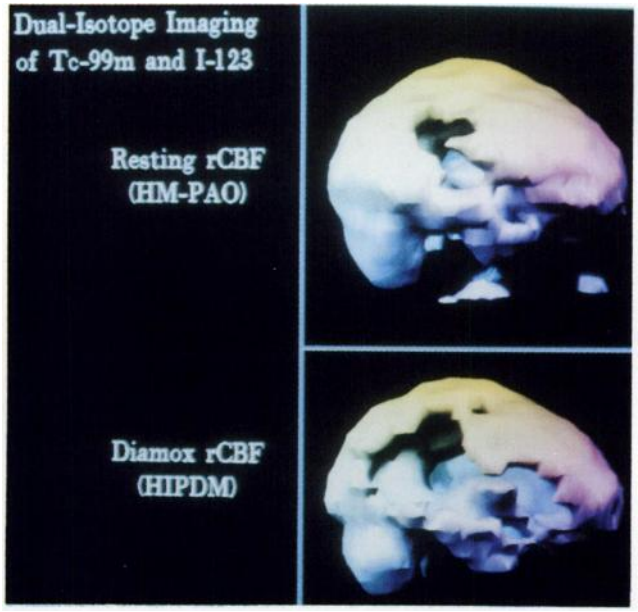

FIGURE 4. Three-dimensional surface-rendered images showing a right frontoparietal resting rCBF deficit with expansion following vasodilation with Diamox in a stroke patient. The difference in affected areas in the resting and vasodilated studies represents the area of failed vasodilatory reserve.

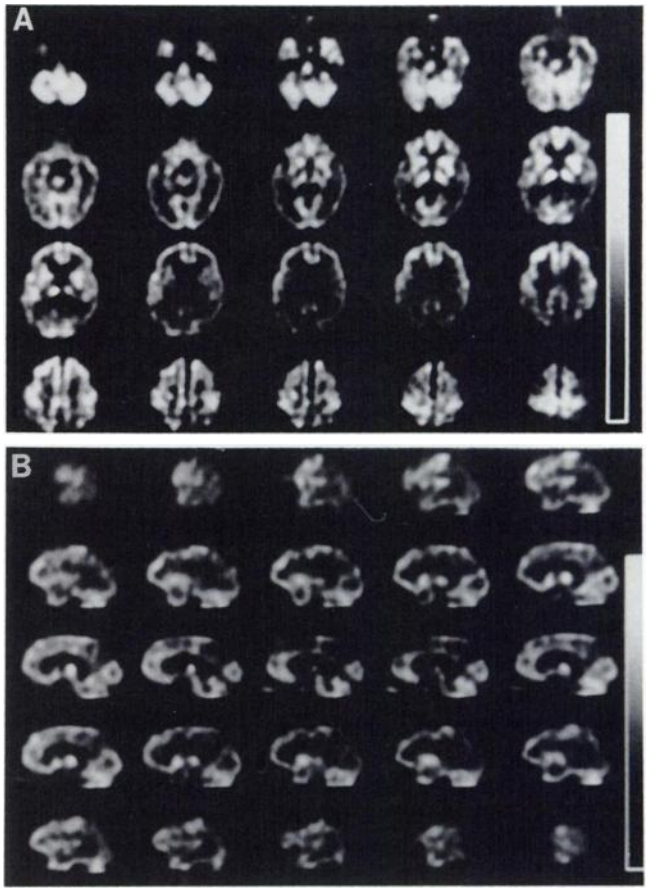

FIGURE 5. Technetium-99m-HMPAO SPECT using the high-resolution ASPECT system. Bilateral temporoparietal perfusion defects in a patient with Alzheimer's disease. Axial (A) and sagittal (B) planes.

DEMENTIA

Alzheimer's Disease

Approximately half of the patients presenting with early clinical symptoms of dementia cannot be accurately diagnosed by clinical criteria. Early diagnosis is important because dementia-like symptoms may mask reversible conditions, such as depression, or treatable diseases, such as vascular dementia. Furthermore, early diagnosis of Alzheimer's disease can avoid the financial and emotional drain that often occurs if the time to final diagnosis is needlessly delayed.

Brain perfusion SPECT is useful in the diagnostic evaluation of patients with memory and cognitive abnormalities (*79*). Initial clinical studies comparing patients with Alzheimer's disease and normal control subjects (*80–87*) or patients with multi-infarct dementia (*88–91*) found that SPECT is highly accurate. In severely impaired patients, sensitivity is 95% or greater (*79,83*). The sensitivity of SPECT in the classification of mildly impaired patients is also high, with rates reported between 80% and 87% (*79, 86,92*).

The predominant finding of bilateral posterior temporal and parietal perfusion defects in these patients is highly predictive of Alzheimer's disease (Fig. 5). In a prospective study of over 100 patients with memory loss, bilateral posterior association cortex defects were detected with ^{99m}Tc-HMPAO SPECT in 65% of the patients with Alzheimer's disease (*93*). This pattern, with or without additional association cortex defects, has a predictive value of over 80% for the diagnosis of Alzheimer's disease.

While bilateral posterior cortical defects are highly predictive in Alzheimer's disease, this scintigraphic pattern has also been described in patients with vascular dementia (*91*), Parkinson's disease (*94,95*), mitochondrial encephalomyopathy (*96*), hypoglycemia (*97*) and carbon monoxide poisoning (*97*). The scintigraphic pattern of Parkinson's disease with dementia cannot be distinguished from that of Alzheimer's disease by visual assessment alone. While Parkinson's disease patients with dementia have a variety of scintigraphic patterns, the most common involves the temporoparietal cortex (*94,95*).

The reduced tracer uptake in the posterior association cortex in patients with Alzheimer's disease is probably due to multiple factors, including reduced rCBF, decreased cortical thickness in the temporoparietal cortex (*98*) and a reduced number of neurons in the affected areas (*99*). Most of the reduced tracer activity is due to reduced regional blood flow, however, particularly in early disease (*100*). In any case, the combined effect of flow reduction and atrophy serve to increase the diagnostic sensitivity of the test, and atrophy corrections are probably not warranted for routine applications.

Patients with Alzheimer's disease can present with other

scintigraphic patterns, although they are less frequent than bilateral posterior cortical defects (*93*). Unilateral temporoparietal defects are not predictive either for or against Alzheimer's disease. With ^{99m}Tc-HMPAO, unilateral posterior defects are seen in 15%–20% of patients with Alzheimer's disease (*93*), significantly more than with [^{123}I] IMP (*80*). Consequently, vascular dementia involving the posterior branches of the middle cerebral artery may resemble Alzheimer's disease when the latter presents as a unilateral pattern.

Some investigators recognize dementia of the frontal type as an entity separate from Alzheimer's disease (*92*), with the former presenting with personality and behavioral changes and with less severe memory deficits. These investigators find that the two dementias can be distinguished scintigraphically, with bilateral frontal or frontotemporal deficits characteristic of frontal lobe dementia. Frontal dementia is considered by many to be a subset of Alzheimer's disease. In either case, bilateral frontal deficits by themselves are not diagnostic and are seen in patients with schizophrenia, depression, progressive supranuclear palsy (usually with basal ganglia involvement) and Pick's disease as well as in Alzheimer's disease and/or frontal lobe dementia.

The probability of Alzheimer's disease with normal perfusion or with perfusion defects outside the temporoparietal cortex is low. The predictive value of a normal scan depends on the clinical setting. When patients are well screened before referral for SPECT, few of them will be without central nervous system disease. In our experience, when patients are screened by a memory disorder clinic, the negative predictive value of a normal study is about 80%. The predictive value will increase as more normal patients are included in the population.

Vascular Dementia

Vascular dementia is related to a number of distinct underlying diseases (*101*). Binswanger's disease or subcortical atherosclerotic encephalopathy involves the microcirculation, presents as white matter disease and is attributed to atherosclerosis of penetrating cerebral arteries. Multi-infarct dementia involves the large vessels and results from large cerebral infarcts. A third disease, a form of multi-infarct dementia but not usually involving large-vessel occlusion, results from multiple small, deep, subcortical lacunar and pericapsular infarctions. Mixed forms of these three vascular diseases often occur. Technetium-99m-HMPAO SPECT appears reasonably accurate for distinguishing vascular dementia from Alzheimer's disease when bilateral temporoparietal defects are present (*82,83*). The scintigraphic pattern of multi-infarct dementia is usually described as multiple asymmetrical perfusion defects, often involving the primary cortex and deep structures. Vascular dementias which involve the subcortical structure are associated with patchy or diffuse patterns of blood flow reduction.

AIDS Dementia Complex

The early clinical signs of AIDS dementia complex (ADC) or HIV encephalopathy are often subtle and may be indistinguishable from depression, psychosis or focal neurologic disease. Since treatment such as zidovudine (AZT) can improve cognitive function in ADC, its early detection is important. Computed tomography (CT) and magnetic resonance imaging (MRI) play a role in diagnosing focal neurologic disease, such as infection or tumor, but are nonspecific for ADC. Brain perfusion SPECT is highly sensitive for the detection of ADC (*102–104*). Early disease is easily separated from normal subjects and non-HIV psychoses (*105–106*). The perfusion pattern is usually described as multifocal or patchy cortical and subcortical hypoperfusion. With high-resolution SPECT, we found a high incidence of cortical defects in ADC, which are most frequent in the frontal, temporal and parietal lobes (*107*) (Fig. 6). Background activity is high, involving more than half of the patients in our series. Basal ganglia involvement is also frequent. A high number of patients have focal areas of increased activity as well. The perfusion pattern improves with ADC therapy (*105*). Brain perfusion SPECT should be applied cautiously in patients with suspected ADC because an identical brain perfusion pattern is seen among chronic cocaine polydrug users (*107*). It is also not clear whether the perfusion pattern is limited to ADC or may be seen with nonspecific changes such as white matter pallor, astrocytic proliferation and mononuclear infiltration which are present in almost all AIDS patients. It may not matter since SPECT imaging may prove to be an indicator of the severity of brain dysfunction and therefore may be quite useful in planning therapy and in evaluating its effectiveness.

EPILEPSY

Functional brain imaging with either SPECT or PET is now a well-established technique to localize the epileptic focus in patients with refractory complex partial seizures

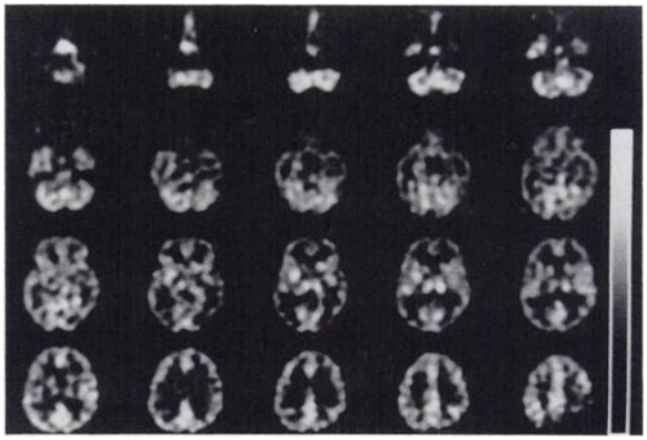

FIGURE 6. Technetium-99m-HMPAO SPECT (axial planes). Multiple small perfusion defects throughout the cerebral cortex in a patient with AIDS dementia complex.

(*108*). From 30% to 60% of patients with complex partial seizures ultimately become refractory to medical treatment and may be referred for surgical removal of a discrete seizure focus. Since most complex partial seizures arise from temporal lobe foci (*109*), temporal lobectomy is the appropriate surgical therapy. Successful excision of well-localized foci leads to elimination of seizures or significantly improved pharmacologic control in 80% of surgical patients (*110*). Traditionally, localization has been performed with scalp, cortical or depth EEG. However, scalp EEG may be misleading in the localization of the primary site of seizure onset because it has inherently low spatial resolution and is fundamentally dependent upon primarily cortical surface effects. Surface electrocorticography is also limited by the area of brain sampled and its sensitivity to and localization of deep-lying generators. Depth EEG can monitor deeper structures but samples only limited regions of brain. Both corticography and depth EEG are extremely invasive and present a surgical risk. Ward has reported that in the United States there are 50,000 patients with medically refractory complex partial seizures possibly benefiting from temporal lobectomy (*111*). Of these, only approximately 500 per year receive surgery, partially due to the difficulty of adequate focus localization.

Interictal SPECT rCBF imaging is the most convenient and cost-effective technique for the localization of a temporal lobe focus in adult patients with medically refractory complex partial seizures. Studies to date would suggest that, when an area of focal temporal lobe hypoperfusion is observed, the need for further studies is minimal (particularly if scalp EEG is concordant).

Partial Complex Seizures

Interictal Studies. Interictal PET studies of glucose metabolism have consistently demonstrated that approximately 70% of patients with complex partial seizures have discrete foci of hypometabolism and that these sites may occur in more than one brain region in the same patient (*112–121*). There is a strong correlation between the area of hypometabolism and the site of electrophysiologic abnormality determined by a combination of electrophysiologic data.

In rCBF studies employing ^{133}Xe SPECT, only 50% demonstrate interictal hypoperfusion (*122–124*). Most often, hypoperfusion is found at the site of the EEG abnormality, but flow deficits are also seen in other remote areas. No specific type of EEG abnormality is associated with reduced rCBF; equal flow reductions were seen in the presence of focal spiking alone, focal spikes and slowing and focal slowing alone (*125*). The first high-resolution interictal scans with SPECT employed [^{123}I]IMP and HIPDM (*126–129*). More recently, interictal scans have been obtained with ^{99m}Tc-HMPAO by a variety of investigators (*130–134*). Interictal SPECT findings with the iodinated amines and ^{99m}Tc-HMPAO show a frequency of abnormal interictal hypoperfusion (70%–75%) similar to PET studies and excellent correlation with EEG localization (Fig. 7). Rowe et al. (*133*) studied 32 patients with HMPAO, 30 of whom had temporal lobe localization by ictal EEG; 18 of 30 patients had focal hypoperfusion at the site of the EEG focus interictally. Devous et al. studied 38 patients with either IMP or HMPAO interictally, and in those patients with EEG-identified foci, approximately 75% had interictal hypoperfusion (*134*).

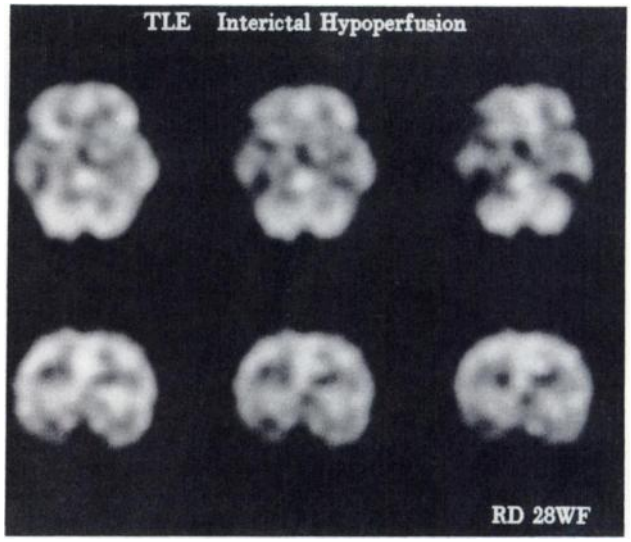

FIGURE 7. Interictal right temporal lobe hypoperfusion in a patient with temporal lobe epilepsy (TLE) on transverse and coronal slices using [^{123}I]IMP. The asymmetry of temporal lobe perfusion is typical of the interictal state in such patients.

Ictal Studies. HIPDM and IMP can be effectively used for ictal studies as long as careful EEG monitoring is used to document seizure onset (Fig. 8). In the postictal phase, cerebral blood flow decouples from glucose metabolism; rCBF remains elevated (*127,135*), while glucose metabo-

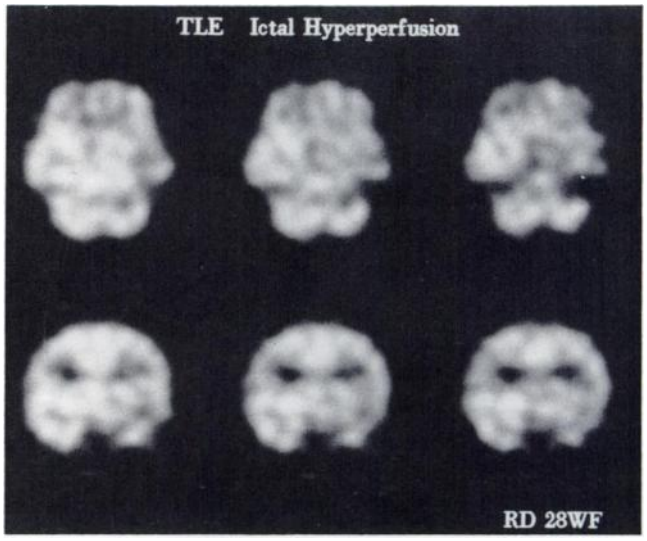

FIGURE 8. Hyperperfusion of the right temporal lobe is shown during an ictus in a patient with temporal lobe epilepsy (TLE). This is the same patient shown in the interictal state in Figure 7. Note the reversal in asymmetry documenting seizure localization to the right temporal lobe.

lism declines rapidly (*118*). In addition, secondary generalization may occur. Ictal studies with iodinated agents have been more successful in identifying seizure foci than interictal studies (*126,128,129,134*). Unfortunately, true ictal studies with HMPAO are nearly impossible to obtain because this compound is unstable in vitro, leading to delays between seizure onset and injection of 5–20 min. In the study by Rowe et al., 22/30 patients with focal EEG findings showed increased postictal HMPAO uptake at the site of the EEG focus (*133*). These data suggest that early postictal studies (within 5 min) may be as effective as true ictal injections.

In a recent review, the combination of all EEG data was localizing in 71% of the patients (*108*). By contrast, functional imaging (SPECT or PET) was localizing in 59% of the interictal studies and 65% of ictal studies. These data suggest that of the patients with EEG-localized seizure foci, 79% were equally well localized by functional brain imaging. It is interesting to note that the localizing power of interictal functional imaging is not substantially different between SPECT and PET, nor is it significantly different between IMP, HIPDM and HMPAO.

Primary Generalized Seizures

There are few data concerning functional abnormalities in generalized seizures (*12,136–138*). These results are consistent with the failure of surface or depth EEG or structural imaging modalities such as CT and MRI to define a specific anatomic region of seizure origin in these patients (*139*). Leroy et al. did not detect quantitative asymmetries in rCBF (*137*) and Theodore et al. found no significant differences in glucose metabolic rates (*136*).

Frontal Lobe Seizures

In recent years, there has been increased interest in partial seizures originating from areas other than the temporal lobe (*140*). Frontal lobe seizures have been difficult to localize using standard EEG technique, and stereotactic depth electrodes have not proven to be as beneficial for localizing the site of the seizure origin as in temporal lobe seizures. The results of surgical treatment of extratemporal partial seizures has been disappointing in comparison to the results of temporal lobe surgery. Functional imaging holds promise for localization of the site of extratemporal seizures, but limited data currently exist. It appears that 60%–70% of subjects with proven extratemporal seizures demonstrate hypometabolism interictally (*141*). These hypometabolic areas appear widespread and are less localized than in temporal lobe seizures.

Structural, Clinical and Cognitive Correlations

Patients with partial and secondarily generalized seizures are much more likely to have structural abnormalities observable on CT or MRI than patients with primary generalized tonic-clonic seizures or absence attacks (*142*). It is not always true that abnormalities detected on structural imaging studies are correlated with the seizure focus defined by clinical or EEG criteria or, for that matter, with functional brain imaging. By far, the most common pathologic finding is mesial temporal sclerosis, which is thought to be the consequence of an older lesion now manifested as a gliotic scar (*143*). A review of SPECT and PET studies demonstrates a 34% incidence of focal MRI abnormalities and a 17% incidence on CT. This is contrasted to a 71% incidence of focal EEG changes and a 59% incidence of focal abnormalities on interictal functional imaging measures (*108*). A few studies demonstrate a close relationship between the severity of interictal rCBF reductions and either clinical symptomatology or cognitive impairment (*144*). Homan et al. compared SPECT and neuropsychological assessments in 50 patients with partial seizures (*145*). Even though rCBF and neuropsychological deficits were relatively mild in many patients, at least one low-flow region matched an area of neuropsychologically impaired function in 43 of 50 patients. There was a significant correlation between areas of visually identified hypoperfusion and neuropsychological impairment ($p < 0.001$). Stepwise discriminate function analyses revealed predictive relationships between deficits on specific neuropsychological tests and visually identified hypoperfusion, particularly in the left and right temporal regions. Similar data were reported by Berent et al. (*146*).

Pediatric Studies

Seizures in children may result from a variety of underlying pathologies. There may be no relationship between clinical symptoms and either electrographic or radiographic findings, and the patients often have unpredictable courses. Functional brain imaging could be useful in understanding clinical pleomorphisms associated with particular diseases, or as a device for subcategorizations useful in predicting progression. Unfortunately, there are only seven published studies concerning functional brain imaging in pediatric epilepsy, excluding case reports and abstracts. Six of these involve PET (*147–152*) and one is an IMP SPECT study (*153*). The only clear conclusion that may be drawn is that more work needs to be done. It is likely, given the adult experience and the limited pediatric results, that functional brain imaging abnormalities will precede structural signs in infants and will likely provide an insight into observed seizure activity. The limited studies available for review suggest of a prognostic as well as a diagnostic role for functional brain imaging in pediatric patients, but such a role is not yet established.

PRIMARY BRAIN TUMORS

Malignant gliomas carry a dismal prognosis due to their aggressive biological behavior. Newer treatment modalities, however, including radiosurgery and brachytherapy, have resulted in increased local control and survival rates (*154*). With aggressive treatment, an increasing number of patients will present with symptoms and signs that may be secondary to recurrent tumor or to radiation changes alone. Establishing the cause of clinical deterioration in malignant glioma patients treated with high dose radiation

is necessary for determining appropriate management. Progressive radiation necrosis requires surgical debulking, while solid tumor recurrence may require adjuvant therapy. CT and MRI are nonspecific and cannot distinguish radiation necrosis from treated tumor (*155,156*). Even CT-guided biopsy may be unreliable. While PET has been useful to assess tumor viability and to differentiate recurrent glioma from radiation change (*157*), it is not readily available in most medical centers.

Thallium-201 localizes in primary and metastatic brain tumors (*158*). Its mechanism of uptake is unknown, but may involve transmembrane transport into viable tumor cells (*159*). When ^{201}Tl tumor uptake was compared to activity in the contralateral hemisphere, high-grade gliomas were differentiated from low-grade lesions (*160, 161*). Since this distinction has both prognostic and therapeutic implications, preoperative ^{201}Tl SPECT may aid in the timing of biopsy or surgery.

Combined ^{201}Tl/^{99m}Tc-HMPAO SPECT is useful for discriminating radiation changes from tumor necrosis as the cause of clinical deterioration in patients with malignant glioma who have also been treated with high dose radiation. While ^{201}Tl-chloride scintigraphy is highly sensitive for identifying recurrent tumors (*162*), in our experience it is insufficiently specific to be clinically useful by itself (*163*). When combined with ^{99m}Tc-HMPAO, however, three patterns of uptake can be identified. High thallium activity (a tumor-to-scalp ratio of greater than 3.5) is highly predictive of solid tumor recurrence in these patients (Fig. 9). When the thallium activity ratio is moderate or low (less than 3.5) and ^{99m}Tc uptake is also low (less than 50% of cerebellar activity), the likelihood of solid tumor recurrence is low. In those patients with moderate thallium uptake and high perfusion, SPECT is not predictive of either tumor or reactive tissue. This method may also prove useful for identifying the appropriate target for stereotactic biopsy excision or ablation once the SPECT and structural image are accurately merged (*25*).

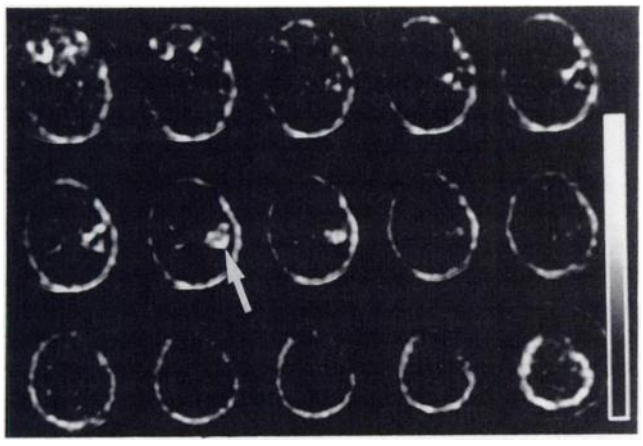

FIGURE 9. Thallium-201 SPECT (axial planes). Horseshoe-shaped region of high ^{201}Tl uptake in a patient with a recurrent glioblastoma in the right temporal lobe following surgery and brachytherapy.

PSYCHIATRIC DISEASE

SPECT applications in psychiatric disorders are not yet clinically useful. We have not yet discovered diagnostic or prognostic functional abnormalities in the major psychiatric diseases. However, SPECT may be of value in identifying unsuspected functional lesions. SPECT may also be useful to rule out organic complications not evident on other diagnostic tests. Promising research into mood disorders, schizophrenia and anxiety disorders suggests that diagnostic and prognostic roles for SPECT may soon emerge.

Depression

Twenty studies in the last 10 years found alterations in cerebral perfusion or metabolism in depressed subjects (*164–183*). Others have reported on effects of medication, electroconvulsive therapy and cognitive tasking in such patients (*184–188*). Unfortunately, findings are inconsistent. There are numerous reasons, including error due to small samples, variations in age and gender distribution, diagnostic heterogeneity, study conditions, severity of depression, and medication status. However, there are consistent indications of reduced global blood flow (gCBF) or glucose metabolism (gCGM), particularly in patients with major depressive disorder (MDD), and possible reductions in the basal ganglia in both bipolar depressed-phase (BP) and MDD samples. There are also suggestions of alterations in the anterior-to-posterior gradient. Studies have reported a relationship between cerebral biochemistry and symptom severity. Baxter recently suggested an emerging consensus for involvement of lateral prefrontal cortex, noting decreased rCGM in lateral prefrontal cortex in depression and elevated rCGM in orbital cortex in obsessive-compulsive disorder (OCD) (*189*). While some conceptual consensus is developing, firm conclusions would be premature. For example, striatal abnormalities, while reported for both disorders, have not been consistently identified.

One explanation for the diversity of findings seen in the existing literature is that no single region of the brain distinguishes depressed individuals from controls or is consistently related over time to the symptomatology observed in depression. For example, Sackeim et al. found that an interacting network of regions explained the topographic distinctions between their BP patients and normal controls and that these regional effects existed separately from global alterations (*181*). Also, Devous et al. recently compared ^{133}Xe SPECT in rCBF in 48 symptomatic MDD patients (13 nonendogenous, 24 endogenous and 11 psychotic) to 48 age- and gender-matched normal controls (*188*). Results revealed a significant age-by-depressive subtype interaction for gCBF and for rCBF ratios. Age effects on rCBF differed not only by region but also among the three diagnostic subtypes. These findings of age effects among depressive subgroups are only one indication of the heterogenous nature of the population. For example,

the notion of global reductions in cerebral blood flow in depression has been both supported and opposed. Such a diversity of results may be explained by examining the endogenous/nonendogenous and psychotic/nonpsychotic patient mixtures in each study.

Obsessive Compulsive Disorder

PET studies have revealed abnormalities in glucose metabolic rates in obsessive compulsive disorder (OCD) patients, but the implicated areas vary from study to study. Baxter et al. have found increased metabolism in the caudate nuclei, orbital gyri, hemispheres and orbital gyrus-to-hemisphere ratio bilaterally (*190,191*). Nordahl et al. did not report global, hemispheric or caudate abnormalities, but did find increased orbital frontal metabolism bilaterally and decreased right parietal and left parieto-occipital metabolism in OCD as compared to normals (*192*). Another conflicting study reports increased metabolism in the right prefrontal cortex and in the left anterior cingulate (*193*). A ^{133}Xe SPECT study in 14 OCD patients found significantly lower mean blood flow, but no regional differences between OCD and matched normals (*194*). Similarly, Nordahl et al. found lower glucose metabolic rates in OCD than in normal controls in most brain regions.

Schizophrenia

Recent reviews suggest that SPECT and PET, as well as the nonimaging ^{133}Xe inhalation probe technique, provide evidence for frontal lobe dysfunction in certain subtypes of schizophrenia (*195,196*). While hypofrontality has been reported frequently (*197–200*), not all investigators have observed it (*201–203*). Inconsistent findings have been attributed to variability in study populations with regard to age, duration of disease, clinical state, subtyping (especially along the paranoid/nonparanoid dimension) and medication status (*204–208*). Frontal lobe dysfunction may be more evident during the performance of cognitive tasks designed for frontal lobe activation (*197,199,207, 209–213*). Hypofrontality also appears to be associated with the negative symptoms of schizophrenia (*195,199*). Temporal lobe abnormalities have also been reported (*199, 209,214*). The combination of both anterior and posterior functional alterations is often expressed as an abnormality in the anterior/posterior gradient. Buchsbaum et al. and others have also reported subcortical abnormalities, particularly on the left side (*198,203,217–221*). Generalized left hemispheric dysfunction (laterality) has also been reported (*195,203,204,222*).

HEAD INJURY

Traumatic brain injury has an overall incidence similar to that of stroke, with a particularly high mortality in the first 48 hr post-trauma (*223*). Proper management of these patients requires an accurate assessment of underlying brain function and, consequently, emission computed tomography has been investigated as a possible monitor. Technetium-99m-HMPAO SPECT has been shown to be more sensitive than CT in detecting abnormalities in patients with a history of traumatic brain injury, particularly in the minor head injury group (*223*). Thus, 42 patients (80%) showed rCBF deficits with SPECT compared with 29 patients (55%) with CT. In addition to its higher sensitivity, SPECT reflects changes in perfusion at an earlier time than CT (*224*). In a preliminary study, patients with large lesions, multiple defects and lesions involving the brain stem appeared to have a worse prognosis than those patients with nonfocal, small lesions, particularly if they involved frontal or occipital lobes. SPECT may also predict the degree of permanent damage and those patients who will develop post-traumatic headache (*225*). Roper et al. has shown that with HMPAO SPECT some patients with traumatic brain injury may have cerebral blood flow equal to that of surrounding brain (*226*). This information may be of prognostic value or may simply indicate luxury perfusion with disassociation between metabolism and flow. At this point, the number of studies of SPECT and traumatic brain injury are small and involve only a few patients, but this application appears promising.

NEURORECEPTOR IMAGING

Neuroreceptor imaging now plays a very limited role in clinical practice. Early clinical trials and the much larger PET experience suggest that useful applications will emerge and that a wide spectrum of radioligands will become available. SPECT ligands have been developed for muscarinic cholinergic receptors (^{123}I-3-quinuclidinyl-4-iodobenzilate, IQNB), the dopamine D-2 receptors ([^{123}I] iodobenzamide, IBZM), the serotonin-2 receptor ([^{123}I] iodoketanserin) and the benzodiazepine receptor (^{123}I-Ro 16-0154m, Iomazenil).

The dopaminergic system plays an important role in the coordination of normal brain function and is a primary action site for neuroleptic drugs for treating schizophrenia and Parkinson's disease. Furthermore, a number of central nervous system diseases, including schizophrenia, tardive dyskinesia, Parkinson's disease and Huntington's chorea, are associated with changes in dopamine receptor density in the brain. Iodine-123-IBZM has been imaged in humans and has a distribution similar to that of positron-labeled D-2 receptor antagonists with localization primarily in the basal ganglia (*227*).

Iomazenil is a specific ligand for benzodiazepine receptors in the human brain (*228*). The highest concentration of this receptor antagonist is in the medial occipital cortex. Iomazenil distribution is altered in partial epilepsy and, in early qualitative imaging studies, appears to be abnormal even when perfusion studies are normal.

Iodine-123-IQNB studies of muscarinic acetylcholine receptor binding in patients with Alzheimer's disease result in images which are similar or less abnormal than images of perfusion in the same patients with Alzheimer's disease (*229,230*). Studies of the muscarinic acetylcholine system

are currently limited by nonspecific ligands such as IQNB, which label most or all of the muscarinic receptor sites and cannot differentiate presynaptic from postsynaptic binding.

A number of problems will have to be overcome if SPECT imaging is to play an important role in the assessment of neurotransmitter function. High spatial resolution will be necessary to quantify absolute tracer concentration. While receptor affinity can be determined from relative measurements of radioactive concentrations (*231*), careful modeling will be necessary to account for radiotracer kinetics and the effect of blood flow on tracer distribution. It is possible, however, that scintigraphic imaging alone may provide enough information to be diagnostically useful, as it has been with perfusion imaging. Furthermore, many neurotransmitters bind to a family of receptors. Unless ligands are developed for specific receptor sites, the full value of this method will not be realized.

CONCLUSION

Substantial literature has emerged over the past decade charting potentially powerful applications of functional brain SPECT in cerebrovascular disease, dementia, epilepsy, cancer and psychiatric disease. Nevertheless, its full potential as a diagnostic tool will emerge only when clearly defined applications demonstrate scintigraphic findings which facilitate critical management decisions. Such applications are now beginning to emerge (Table 1) and more will become evident as well-designed clinical trials of efficacy and patient outcome establish its utility (Table 2). Functional tests such as perfusion SPECT require careful and imaginative investigations to determine the proper diagnostic role of the physiological information that they provide as well as close cooperation between nuclear medicine physicians and their clinical colleagues to assure that the most relevant clinical questions are being answered. Properly approached, functional SPECT provides a unique window to explore the hemodynamic and biochemical consequences of diseases that affect the brain.

TABLE 1
Widely Accepted Uses of Brain SPECT

Alzheimer's disease
Acute stroke
Transient ischemic attacks
Epilepsy
Recurrent primary tumor
Head trauma

TABLE 2
Potential Applications of Brain SPECT

Cerebrovascular disease
Delineation of stroke subtypes
Cerebrovascular reserve
Stroke prognosis
Stroke risk
Subarachnoid hemorrhage prognosis
Dementia
AIDS dementia complex
Huntington's disease
Dementia severity, prognosis and treatment
Psychiatric disease
Schizophrenia
Depression
Anxiety disorders
Parkinson's disease
Substance abuse
CNS involvement in systemic disease
Chronic fatigue syndrome
Lupus
Others
Pharmacologic and cognitive challenge tests

REFERENCES

1. Kuhl DE, Barrco JR, Huang SC, et al. Quantifying local cerebral blood flow with N-isopropyl-p-I-123 iodoamphetamine (IMP) tomography. *J Nucl Med* 1982;23:196–203.
2. Winchell HS, Baldwin RM, Lin TH. Development of I-123-labeled amines for brain studies: localization of I-123 iodophenyalkyl amines in rat brain. *J Nucl Med* 1980;21:947–952.
3. Hill TC, Holman BL, Lovett R, et al. Initial experience with SPECT (single photon emission computerized tomography) of the brain using N-isopropyl I-123 p-iodoamphetamine. *J Nucl Med* 1982;23:191–195.
4. Holman BL, Lee RGL, Hill TC, Lovett RD, Lister-James J. A comparison of two cerebral perfusion tracers. N-isopropyl-I-123 p-iodoamphetamine and I-123 HIPDM in the human. *J Nucl Med* 1984;25:25–30.
5. Ell PJ, Hocknell JML, Jarritt PH, et al. A Tc-99m-labeled radiotracer for the investigation of cerebral vascular disease. *Nucl Med Commun* 1985; 6:437–441.
6. Anderson AR, Friberg H, Knudsen KMB, et al. Extraction of Tc-99m-d,l,HM-PAO across the blood-brain barrier. *J Cereb Blood Flow and Metab* 1988;8:S44–S51.
7. Neirinckx RD, Burke JF, Harrison RC, Forster AM, Andersen AR, Lassen NA. The retention mechanism of Tc-99m HMPAO: intracellular reaction with glutathione. *J Cereb Blood Flow Metab* 1988;8:S4–S12.
8. Moretti J-L, Defer G, Cinotti L, et al. "Luxury-perfusion" with Tc-99m-HMPAO and I-123-IMP SPECT imaging during the subacute phase of stroke. *Eur J Nucl Med* 1990;16:17–22.
9. Holman BL, Hellman RS, Goldsmith SJ, et al. Biodistribution, dosimetry, and clinical evaluation of technetium-99m ethyl cysteinate dimer in normal subjects and in patients with chronic cerebral infarction. *J Nucl Med* 1989;30:1018–1025.
10. Walovitch RC, Hill TC, Garrity ST, et al. Characterization of technetium-99m-l, 1-ECD for brain perfusion imaging. Part I. Pharmacology of technetium-99m ECD in non-human primates. *J Nucl Med* 1989;30: 1892–1901.
11. Obrist WD, Thompson HK, Wang HS, Wilkinson WF. Regional cerebral blood flow estimated by xenon-133 inhalation. *Stroke* 1975;6:245–256.
12. Devous MD Sr, Stokely EM, Bonte FJ. Quantitative imaging of regional cerebral blood flow by dynamic single-photon tomography. In: Holman BL, ed. *Radionuclide Imaging of the Brain.* New York: Churchill Livingstone; 1985:135–162.
13. Kimura K, Hashikawa K, Etani H, et al. A new apparatus for brain imaging: four-head rotating gamma camera single-photon emission computed tomography. *J Nucl Med* 1990;31:603–609.
14. Rogers WL, Clinthorne NH, Stamos J, et al. Performance evaluation of SPRINT, a single-photon ring tomograph for brain imaging. *J Nucl Med* 1984;25:1013–1018.
15. Kanno I, Uemura K, Miyura S, Miyura Y. HEADTOME: a hybrid emission tomograph for single-photon and positron emission imaging of the brain. *J Comput Assist Tomogr* 1981;5:216–226.
16. Stoddart HF, Stoddart HA. A new development in single-gamma transaxial tomography. Union Carbide focused collimator scanner. *IEEE*

Trans Nucl Sci 1979;26:2710–2712.
17. Kirsch C-M, Moore SC, Zimmerman RE, English RJ, Holman BL. Characteristics of a scanning, multidetector, single-photon ECT body imager. *J Nucl Med* 1981;22:726–731.
18. Hill TC, Stoddart HF, Doherty MD, Alpert NM, Wolfe AP. Simultaneous SPECT acquisition of CBF and metabolism. *J Nucl Med* 1988;29:876.
19. Devous MD Sr, Bonte FJ. Initial evaluation of cerebral blood flow imaging with a high-resolution, high-sensitivity three-headed SPECT system (PRISM). *J Nucl Med* 1988;29:912.
20. Logan KW, Holmes RA. Missouri University Multiplane Imager (MUMPI): a high sensitivity rapid dynamic ECT brain imager. *J Nucl Med* 1984;25:P105.
21. Smith AP, Genna S. Imaging characteristics of a single-crystal ring camera for dedicated brain SPECT. *J Nucl Med* 1989;30:796.
22. Holman BL, Carvalho PA, Zimmerman RE, et al. Brain perfusion SPECT using an annular single crystal camera: initial clinical experience. *J Nucl Med* 1990;31:1456–1461.
23. Holman BL, Zimmerman RE, Johnson KA, et al. Computer-assisted superimposition of magnetic resonance and high-resolution technetium-99m-HMPAO and thallium-201 SPECT of the brain. *J Nucl Med* 1991; 32:1478–1484.
24. Devous MD Sr, Gassaway SK. Simultaneous SPECT imaging of Tc-99m and I-123-labeled brain agents in patients using the PRISM™ scanner. *J Nucl Med* 1990;31:877.
25. Devous MD Sr, Payne JK, Lowe JL. Dual-isotope SPECT imaging of resting rCBF and cerebrovascular reserve [Abstract]. *J Nucl Med* 1991; 32:972.
26. Hellman RS, Tikofsky RS. An overview of the contributions of regional cerebral blood flow studies in cerebrovascular disease. Is there a role for single photon emission computed tomography? *Semin Nucl Med* 1990; 20:303–324.
27. Alavi A, Hirsch LJ. Studies of central nervous system disorders with single photon emission computed tomography and positron emission tomography: evolution over the past two decades. *Semin Nucl Med* 1991;21: 58–81.
28. Fayad PB, Brass LM. Single photon emission computed tomography in cerebrovascular disease. *Stroke* 1991;22:950–954.
29. Caplan LR. Question-driven technology assessment: SPECT as an example. *Neurology* 1991;41:187–191.
30. Brass LM, Rattner Z. Single photon emission computed tomography in cerebral vascular disease. In: Weber DA, Devous MD, Tikofsky RS, eds. *Workshop on Brain SPECT perfusion imaging: optimizing imaging acquisition and processing.* DOE CONF-9110368, 1992:77–88.
31. Fieschi C, Argentino C, Lenzi GL, Sacchetti ML, Toni D, Bozzao L. Clinical and instrumental evaluation of patients with ischemic stroke within the first six hours. *J Neurol Psychiatry* 1989;91:311–322.
32. Bose A, Pacia SB, Fayad P, Smith EO, Brass LM, Hoffer P. Cerebral blood flow imaging compared to CT during the initial 24 hours of cerebral infarction. *Neurology* 1990;40:190.
33. Podreka I, Suess E, Goldenberg G, et al. Initial experience with technetium-99m HM-PAO brain SPECT. *J Nucl Med* 1987;28:1657–1666.
34. De Roo M, Mortelmans L, Devos P, et al. Clinical experience with Tc-99m HM-PAO high resolution SPECT of the brain in patients with cerebrovascular accidents. *Eur J Nucl Med* 1989;15:9–15.
35. Lassen NA. The luxury-perfusion syndrome and its possible relation to metabolic acidosis located with the brain. *Lancet* 1966;2:1113–1115.
36. Pantano P, Baron JC, Samson Y, Bousser MG, Derouesne C, Comar D. Crossed cerebellar diaschisis. Further studies. *Brain* 1986;109:677–694.
37. Kushner M, Alavi A, Reivich M, Dann R, Burke A, Robinson G. Contralateral cerebellar hypometabolism following cerebral insult: a positron emission tomographic study. *Ann Neurol* 1984;15:425–434.
38. Gibbs JM, Wise RSJ, Leenders KL, Jones T. Evaluation of cerebral perfusion reserve in patients with carotid-artery occlusion. *Lancet* 1984; 8372:310–314.
39. Buell U, Braun H, Ferbert A, Stirner H, Weiller C, Ringelstein EB. Combined SPECT imaging of regional cerebral blood flow (^{99m}Tc-hexamethyl-propyleneamine oxime, HM-PAO) and blood volume (^{99m}Tc-RBC) to assess regional cerebral perfusion reserve in patients with cerebrovascular disease. *Nuklear Medizin* 1988;27:51–56.
40. Devous MD Sr, Arora GD. Direct measurement of rOER, rCBF, and rCBV define a relationship between rOER and the rCBF/rCBV ratio in acute stroke. *J Nucl Med* 1991;32(5):960.
41. Vorstrup S, Boysen G, Brun B, Engell HC. Evaluation of the regional cerebral vasodilatory capacity before carotid endarterectomy by the accetazolamide test. *Neurol Res* 1987;9:10–18.
42. Tikofsky RS, Hellman RS. Brain single photon emission computed tomography: New activation and intervention studies. *Semin Nucl Med* 1991;21:40–57.
43. Bonte FJ, Devous MD Sr, Reisch JS. The effect of acetazolamide on regional cerebral blood flow in normal human subjects as measured by single photon emission computed tomography. *Invest Radiol* 1988;23: 564–568.
44. Heiss W, Zeiler K, Havelec L, Reisner T, Bruck J. Long-term prognosis in stroke related to cerebral blood flow. *Arch Neurol* 1988;34:671–676.
45. Nagata K, Yunoki K, Kabe S, Suzuki A, Araki G. Regional cerebral blood flow correlates of aphasia outcome in cerebral hemorrhage and cerebral infarction. *Stroke* 1986;17:417–423.
46. Kushner M, Reivich M, Fieschi C, et al. Metabolic and clinical correlates of acute ischemic infarction. *Neurology* 1987;37:1103–1110.
47. Defer G, Moretti JL, Cesaro P, Sergent A, Raynaud C, Degos JD. Early and delayed SPECT using N-isopropyl p-iodoamphetamine iodine-123 in cerebral ischemia. A prognostic index for clinical recovery. *Arch Neurol* 1987;44:715–718.
48. Lee RGL, Hill TC, Holman BL, Royal HD, O'Leary DH, Clouse ME. Predictive value of perfusion defect size using N-isopropyl-(I-23)-p-iodoamphetamine emission tomography in acute stroke. *J Neurosurg* 1984; 61:449–452.
49. Demeurisse G, Verhas M, Capon A, Paternot J. Lack of evolution of the cerebral blood flow during clinical recovery of a stroke. *Stroke* 1983;14: 77–81.
50. Hayman LA, Taber KH, Jhingran SG, Killian JM, Carroll RG. Cerebral infarction. Diagnosis and assessment of prognosis by using ^{123}IMP-SPECT and CT. *AJNR* 1989;10:557–562.
51. Vallar G, Perani D, Cappa SF, Messa C, Lenzi GL, Fazio F. Recovery from aphasia and neglect after subcortical stroke: neuropsychological and cerebral perfusion study. *J Neurol Neurosurg Psychiatry* 1988;51: 1269–1276.
52. Mountz JM, Modell JG, Foster NL, et al. Prognostication of recovery following stroke using the comparison of CT and technetium-99m HM-PAO SPECT. *J Nucl Med* 1990;31:61–66.
53. Limburg M, Van Royen EA, Hijdra A, Verbeeten B Jr. rCBF-SPECT in brain infarction: when does it predict outcome? *J Nucl Med* 1991;32: 382–387.
54. Bushnell DL, Gupta S, Micoch AG, Barnes WE. Prediction of language and neurological recovery after cerebral infarction with SPECT imaging using N-isopropyl-(I-123)-p-iodoamphetamine. *Arch Neurol* 1989;46: 665–669.
55. Giubilei F, Lenzi GL, DiPiero V, et al. Predictive value of brain perfusion single-photon emission computed tomography in acute cerebral ischemia. *Stroke* 1990;21:895–900.
56. Nakano S, Kinoshita K, Jinnouchi S, Hiroaki H, Watanabe K. Comparative study of regional cerebral blood flow images by SPECT using xenon-133, iodine-123 IMP and technetium-99m HM-PAO. *J Nucl Med* 1989; 30:157–164.
57. Yonekura Y, Nishizawa S, Mukai T, et al. SPECT with [^{99m}Tc]-d,l hexamethyl propylene amine oxime (HM-PAO) compared with regional cerebral blood flow measured by PET. Effects of linearization. *J Cereb Blood Flow Metab* 1988;8:S82–S89.
58. Hayashita K, Nishimura T, Imakita S, Vehara T. Filling out phenomenon with technetium-99m HM-PAO brain SPECT at the site of mild cerebral ischemia. *J Nucl Med* 1989;30:591–598.
59. Crow W, Guinto FC Jr. Limitations of CT in the evaluation of transient ischemic attacks. *Tex Med J* 1982;78:65–71.
60. Chollet F, Celsis P, Clanet M, Guiraud CB, Rascol A, Marc VJP. SPECT study of cerebral blood flow reactivity after acetazolamide in patients with transient ischemic attacks. *Stroke* 1989;20:458–464.
61. Bogousslavsky J, Delaloye-Bischof A, Regli F, Delaloye B. Prolonged hypoperfusion and early stroke after transient ischemic attack. *Stroke* 1990;21:40–46.
62. Brust JCM. Transient ischemic attacks: Natural history and anticoagulation. *Neurology* 1977;27:701–707.
63. Hartmann A. Prolonged disturbances of regional cerebral blood flow in transient ischemic attacks. *Stroke* 1985;16:932–939.
64. Devous MD Sr, Batjer HH, Ajmani AK, Samson DS, Bonte FJ. SPECT measurements of cerebrovascular reserve in patients with hemodynamic risk. *J Nucl Med* 1988;29:911.
65. Voldby B. Alterations in vasomotor reactivity in subarachnoid hemorrhage. In: Wood JH, ed. *Cerebral Blood Flow.* New York, NY: McGraw-Hill; 1987:402–412.
66. Biller J, Godersky JC, Adams HP Jr. Management of aneurysmal sub-

arachnoid hemorrhage. *Curr Concepts Cerebrovas Dis Stroke* 1988;23: 13–18.
67. Powers WJ, Grubb RL Jr, Baker RP, Mintun MA, Raichle ME. Regional cerebral blood flow and metabolism in reversible ischemia due to vasospasm. Determination by positron emission tomography. *J Neurosurg* 1985;62:539–546.
68. Grubb RL, Raichle ME, Eichling JO, Gado MH. Effects of subarachnoid hemorrhage on cerebral blood volume, blood flow and oxygen utilization in humans. *J Neurosurg* 1977;46:446–453.
69. Davis S, Andrews J, Lichtenstein M, et al. A single-photon emission computed tomography study of hypoperfusion after subarachnoid hemorrhage. *Stroke* 1990;21:252–259.
70. Caplan LR, Brass LM, DeWitt LD, et al. Transcranial Doppler ultrasound. Present status. *Neurology* 1990;40:696–700.
71. Samson D. Surgical treatment of intracranial arteriovenous malformations. *Tex Med J* 1983;79:52–57.
72. Homan RW, Devous MD Sr, Stokely EM, Bonte FJ. Quantification of intracerebral steal in patients with arteriovenous malformation. *Arch Neurol* 1986;43:779–785.
73. Batjer HH, Devous MD Sr, Seibert GB, et al. Intracranial arteriovenous malformation. Relationships between clinical and radiographic factors and ipsilateral steal severity. *Neurosurgery* 1988;23:322–328.
74. Batjer HH, Devous MD Sr, Meyer YJ, et al. Cerebrovascular hemodynamics in arteriovenous malformation complicated by normal perfusion pressure breakthrough. *Neurosurgery* 1988;22:503–509.
75. Batjer HH, Devous MD Sr, Seibert GB, Purdy PD, Bonte FJ. Intracranial arteriovenous malformation. Relationship between clinical factors and surgical complications. *Neurosurgery* 1989;24:74–79.
76. Devous MD Sr, Batjer HH, Mickey B, Samson DS, White SR, Bonte FJ. Dynamic SPECT measurements of vasodilatory reserve in regions of cerebral steal in patients with arteriovenous malformations. *J Cereb Blood Flow Metab* 1987;7:S200.
77. Batjer HH, Devous MD Sr. The use of acetazolamide-enhanced rCBF measurement to predict risk to AVM patients. *Neurosurgery* 1992: in press.
78. Powers WJ. Cerebral hemodynamics in ischemic cerebrovascular disease. *Ann Neurol* 1991;29:231–240.
79. Johnson KA, Holman BL, Rosen TJ, Nagel JS, English RJ, Growdon JH. Iofetamine I-123 single photon emission computed tomography is accurate in the diagnosis of Alzheimer's disease. *Arch Intern Med* 1990; 150:752–756.
80. Cohen MB, Graham LS, Lake R, et al. Diagnosis of Alzheimer's disease and multiple infarct dementia by tomographic imaging of iodine-123 IMP. *J Nucl Med* 1986;27:769–774.
81. Sharp P, Gemmell H, Cherryman G, Besson J, Crawford J, Smith F. Application of iodine-123-labeled isopropylamphetamine imaging to the study of dementia. *J Nucl Med* 1986;27:761–768.
82. Smith FW, Gemmell HG, Sharp PF. The use of Tc-99m-HM-PAO for the diagnosis of dementia. *Nucl Med Commun* 1987;8:525–533.
83. Jagust WJ, Budinger TF, Reed BR. The diagnosis of dementia with single photon emission computed tomography. *Arch Neurol* 1987;44:258–262.
84. Neary D, Snowden JS, Shields RA, et al. Single photon emission tomography using Tc-99m-HM-PAO in the investigation of dementia. *J Neurol Neurosurg Psychiatry* 1987;50:1101–1109.
85. Johnson KA, Mueller ST, Walshe TM, English RJ, Holman BL. Cerebral perfusion imaging in Alzheimer's disease: use of single photon emission computed tomography and iofetamine hydrochloride I-123. *Arch Neurol* 1987;44:165–168.
86. Perani D, DiPiero V, Vallar G, et al. Technetium-99m HM-PAO SPECT study of regional cerebral perfusion in early Alzheimer's disease. *J Nucl Med* 1988;29:1507–1514.
87. Bonte FJ, Ross ED, Chehabi HH, Devous MD. SPECT study of regional cerebral blood flow in Alzheimer's disease. *J Comput Assist Tomogr* 1986; 10:579–583.
88. Testa HJ, Snowden JS, Neary D, et al. The use of Tc-99m HM-PAO in the diagnosis of primary degenerative dementia. *J Cereb Blood Flow Metab* 1988;8:S123–S126.
89. Hellman RS, Tikofsky RS, Collier BD, et al. Alzheimer's disease: quantitative analysis of I-123-iodoamphetamine SPECT brain imaging. *Radiology* 1989;172:183–188.
90. Deutsch G, Tweedy JR. Cerebral blood flow in severity-matched Alzheimer and multi-infarct patients. *Neurology* 1987;37:431–438.
91. Launes J, Sulkava R, Erkinjuntti T, et al. Tc-99m HMPAO SPECT in suspected dementia. *Nucl Med Commun* 1991;12:757–765.
92. Bonte FJ, Hom J, Tintner R, Weiner MF. Single photon tomography in Alzheimer's disease and the dementias. *Semin Nuc Med* 1990;20: 342–352.
93. Holman BL, Johnson KA, Garada B, Carvalho PA, Satlin A. The scintigraphic appearance of Alzheimer's disease: a prospective study using technetium-99m HMPAO SPECT. *J Nucl Med* 1992;33:181–185.
94. Pizzolato G, Dam M, Borsato N, et al. Tc-99m-HM-PAO SPECT in Parkinson's disease. *J Cereb Blood Flow Metab* 1988;8:S101–S108.
95. Nagel JS, Ichise M, Holman BL. The scintigraphic evaluation of Huntington's disease and other movement disorders using single photon emission computed tomography perfusion brain scans. *Semin Nucl Med* 1991; 21:11–23.
96. Grunwald F, Zierz S, Broich K, Schumacher S, Bockisch A, Biersack HJ. HMPAO-SPECT imaging resembling Alzheimer-type dementia in mitochondrial encephalomyopathy with lactic acidosis and stroke-like episodes (MELAS). *J Nucl Med* 1990;31:1740–1742.
97. Kuwabara Y, Ichiya Y, Otsuka M, et al. Differential diagnosis of bilateral parietal abnormalities in I-123 IMP SPECT imaging. *Clin Nucl Med* 1990;15:893–899.
98. Herscovitch P, Auchus AP, Gado M, Chi D, Raichle ME. Correction of positron emission tomography data for cerebral atrophy. *J Cereb Blood Flow Metab* 1986;6:120–124.
99. Brun A, Englund E. Regional pattern of degeneration in Alzheimer's disease: neuronal loss and histopathological grading. *Histopathology* 1981; 5:549–564.
100. Frieldland RP, Brun A, Budinger TF. Pathological and positron emission tomographic correlations in Alzheimer's disease. *Lancet* 1985;1:228.
101. Buell U, Costa DC, Kirsch G, Moretti JL, Van Royen EA, Schober O. The investigation of dementia with single photon emission tomography. *Nucl Med Commun* 1990;11:823–841.
102. Pohl P, Vogl G, Fill H, Rossler H, Zangerle R, Gerstenbrand F. Single photon emission computed tomography in AIDS dementia complex. *J Nucl Med* 1988;29:1382–1386.
103. Tran Dink YR, Mamo H, Cervoni C, Saimot AC. Disturbances in the cerebral perfusion of human immune deficiency virus-1 seropositive asymptomatic subjects: a quantitative tomography study of 18 cases. *J Nucl Med* 1990;31:1601–1607.
104. Ell PJ, Costa DC, Harrison M. Imaging cerebral damage in HIV infection. *Lancet* 1987;2:569–570.
105. Masdeu JC, Yudd A, Van Heertum RL, et al. Single photon emission computed tomography in human immunodeficiency virus encephalopathy: a preliminary report. *J Nucl Med* 1991;32:1471–1475.
106. Schielke E, Tatsch K, Pfister HW, et al. Reduced cerebral blood flow in early stages of human immunodeficiency virus infection. *Arch Neurol* 1990;47:1342–1345.
107. Holman BL, Garada B, Johnson KA, et al. A comparison of brain perfusion SPECT in cocaine abuse and AIDS dementia complex. *J Nucl Med* 1992;33:1312–1315.
108. Devous MD Sr, Leroy RF, Homan RW. Single photon emission computed tomography in epilepsy. *Semin Nucl Med* 1990;20:325–341.
109. Williamson PD, Wieser HG, Delgado-Escueta AV. Clinical characteristics of partial seizures. In: Engel J Jr, ed. *Surgical treatment of the epilepsies.* New York, NY: Raven Press; 1987:101–120.
110. Engel J Jr. Outcome with respect to epileptic seizures. In: Engel J Jr, ed. *Surgical treatment of the epilepsies.* New York, NY: Raven Press; 1987: 553–571.
111. Ward AA. Perspectives for surgical therapy of epilepsy. In: Ward AA, Penry JK, Purpura D, eds. *Epilepsy* (ARNMD 61). New York, NY: Raven Press; 1983:371–390.
112. Kuhl DE, Engel J Jr, Phelps ME, Selin C. Epileptic patterns of local cerebral metabolism and perfusion in humans determined by emission computed tomography of ^{18}FDG and $^{13}NH_3$. *Ann Neurol* 1980;8: 348–360.
113. Engel J Jr, Kuhl DE, Phelps ME, Mazziotta JC. Interictal cerebral glucose metabolism in partial epilepsy and its relation to EEG changes. *Ann Neurol* 1982;12:510–517.
114. Engel J Jr, Brown WJ, Kuhl DE, Phelps ME, Mazziotta JC, Crandall PH. Pathological findings underlying focal temporal lobe hypometabolism in partial epilepsy. *Ann Neurol* 1982;12:518–528.
115. Engel J Jr, Kuhl DE, Phelps ME, Crandall PH. Comparative localization of the epileptic foci in partial epilepsy by PCT and EEG. *Ann Neurol* 1982;12:529–537.
116. Theodore W, Newmark M, Sato S, et al. F-18-fluorodeoxyglucose positron emission tomography in refractory complex partial seizures. *Ann Neurol* 1983;14:429–437.
117. Bernardi S, Trimble MR, Fracowiak RSJ, Wise RJS, Jones T. An interictal

study of partial epilepsy using positron emission tomography and the oxygen-15 inhalation technique. *J Neurol Neurosurg Psychiatry* 1983; 46:473–477.
118. Mazziotta JC, Engel J Jr. The use and impact of positron computed tomography scanning in epilepsy. *Epilepsia* 1984;25(Suppl 2):S86–S104.
119. Theodore WH, Fishbein D, Dubinsky R. Patterns of cerebral glucose metabolism in patients with partial seizures. *Neurology* 1988;38:1201–1206.
120. Engel J Jr, Kuhl DE, Phelps ME. Patterns of human local cerebral metabolism during epileptic seizures. *Science* 1982;218:64–66.
121. Depresseux JC, Franck G, Sadzot B. Regional cerebral blood flow and oxygen uptake rate in human focal epilepsy. In: Baldy-Moulinier M, Ingvar DH, Meldrum BS, eds. *Current problems in epilepsy: I. cerebral blood flow, metabolism and epilepsy.* London: John Libbey; 1984:76–81.
122. Bonte FJ, Stokely EM, Devous MD Sr, Homan RW. Single-photon tomographic study of regional cerebral blood flow in epilepsy. A preliminary report. *Arch Neurol* 1983;40:267–271.
123. Bonte FJ, Devous MD Sr, Stokely EM, Homan RW. Single-photon tomographic determination of regional cerebral blood flow in epilepsy. *AJNR* 1983;4:544–546.
124. Bonte FJ, Devous MD Sr, Stokely EM, Homan RW, Paulman RG. Single-photon computed tomographic determination of regional brain blood flow in the seizure disorders. *Am J Physiol Imaging* 1988;3: 30–31.
125. Homan RW, Devous MD Sr, Stokely EM, Bonte FJ. Correlation of EEG findings and cerebral blood flow in patients with partial seizures. *Neurology* 1984;34(Suppl 1):124.
126. Magistretti PL, Uren RF. Cerebral blood flow patterns in epilepsy. In: Nistico G, DiPerri R, Meinardi H, eds. *Epilepsy: an update on research and therapy.* New York, NY: Allan R. Liss; 1983:241–247.
127. Lee BI, Markand ON, Siddiqui AR, et al. Single photon emission computed tomography (SPECT) brain imaging using N,N,N′-trimethyl-N′-(2-hydroxy-3-methyl-5-^{123}I-iodobenzyl)-1,3-propanediamine 2 HCl (HIPDM): Intractable complex partial seizures. *Neurology* 1986;36: 1471–1477.
128. Lee BI, Markand ON, Wellman HN, et al. HIPDM single photon emission computed tomography brain imaging in partial onset secondarily generalized tonic-clonic seizures. *Epilepsia* 1987;28:305–311.
129. Lee BI, Markand ON, Wellman HN, et al. HIPDM-SPECT in patients with medically intractable complex partial seizures. Ictal study. *Arch Neurol* 1988;45:397–402.
130. Stefan H, Kuhnen C, Biersack HJ, Reichmann K. Initial experience with ^{99m}Tc hexamethyl-propylene amine oxime (HM-PAO) single photon emission computed tomography (SPECT) in patients with focal epilepsy. *Epilepsy Res* 1987;1:134–138.
131. Andersen AR, Gram L, Kjaer L, et al. SPECT in partial epilepsy: Identifying side of the focus. *Acta Neurol Scand* 1988;117:90–95.
132. Ryding E, Rosen I, Elmqvist B, Ingvar DH. SPECT measurements with ^{99m}Tc-HMPAO in focal epilepsy. *J Cereb Blood Flow Metab* 1988;8: S95–S100.
133. Rowe CC, Berkovic SF, Sia STB, et al. Localization of epileptic foci with post ictal single photon emission computed tomography. *Ann Neurol* 1989;26:660–668.
134. Devous MD Sr, Leroy RF. Comparison of interictal and ictal regional cerebral blood flow findings with scalp and depth electrode seizure focus localization. *J Cereb Blood Flow Metab* 1989;9(suppl 1):S91.
135. Howse PC, Caronna JJ, Duffy TE, Plum F. Cerebral energy metabolism, pH and blood flow during seizures in cat. *Am J Physiol* 1974;227: 1444–1451.
136. Theodore W, Brooks R, Margolin R, et al. Positron emission tomography in generalized seizures. *Neurology* 1985;35:684–690.
137. Leroy RF, Devous MD, Ajmani AK, Rao KK, Bonte FJ. Regional cerebral blood flow determined by xenon-133 inhalation and SPECT scan among epileptics with primary generalized seizures. *Neurology* 1987; 37(suppl 1):102.
138. Mazziotta JC, Engel J Jr. The use and impact of positron computed tomography scanning in epilepsy. *Epilepsia* 1984;25:S86–S104.
139. Gloor P. Generalized epilepsy with spike-and-wave discharge: a reinterpretation of its electrographic and clinical manifestations. *Epilepsia* 1979; 20:517–588.
140. Williamson, PD, Spencer DD, Spencer SS, Novelly RA, Mattson RH. Complex partial seizures of frontal lobe origin. *Ann Neurol* 1985;18: 497–504.
141. Swartz BE, Halgren E, Delgado-Escueta AV, et al. Neuroimaging in patients with seizures of probable frontal lobe origin. *Epilepsia* 1989;30: 547–588.
142. Theodore WH. Neuroimaging. *Neurol Clin* 1986;4:645–668.
143. Falconer MA. Mesial temporal (Ammon's horn) sclerosis as a common cause of epilepsy: etiology, treatment and prevention. *Lancet* 1974;ii: 767–770.
144. Valmier J, Touchon J, Daures P, Zanca M, Baldy-Moulinier M. Correlations between cerebral blood flow variations and clinical parameters in temporal lobe epilepsy: an interictal study. *J Neurol Neurosurg Psychiatry* 1987;50:1306–1311.
145. Homan RW, Paulman RG, Devous MD Sr, Walker P, Jennings LW, Bonte FJ. Cognitive function and regional cerebral blood flow in partial seizures. *Arch Neurol* 1989;46:964–970.
146. Berent S, Sackellares JC, Abou-Khalil B, et al. PET studies of cerebral glucose metabolic activity in temporal lobe epilepsy. The functional implications of lateralized hypometabolism. *Neurology* 1986;36: 337–338.
147. Chugani HT, Mazziotta JC, Engel J Jr, Phelps ME. The Lennox-Gastaut syndrome: Metabolic subtypes determined by 2-deoxy-2[^{18}F]fluoro-D-glucose positron emission tomography. *Ann Neurol* 1987;21:4–13.
148. Theodore WH, Rose D, Patronas N, et al. Cerebral glucose metabolism in the Lennox-Gastaut syndrome. *Ann Neurol* 1987;21:14–21.
149. Yanai K, Iinuma K, Matsuzawa T, et al. Cerebral glucose utilization in pediatric neurological disorders determined by positron emission tomography. *Eur J Nucl Med* 1987;13:292–296.
150. Chugani HT, Mazziotta JC, Phelps ME. Sturge-Weber syndrome: a study of cerebral glucose utilization with positron emission tomography. *J Pediatr* 1989;114:244–253.
151. Engel J Jr, Lubens P, Kuhl DE, Phelps ME. Local cerebral metabolic rate for glucose during petit mal absences. *Ann Neurol* 1985;17:121–128.
152. Chugani HT, Shewmon DA, Peacock WJ, Shields WD, Mazziotta JC, Phelps ME. Surgical treatment of intractable neonatal-onset seizures: the role of positron emission tomography. *Neurology* 1988;38:1178–1188.
153. Denays R, Rubenstein M, Ham H, Piepsz A, Noel P. Single photon emission computed tomography in seizure disorders. *Arch Dis Child* 1988; 63:1184–1188.
154. Loeffler JS, Alexander E III. The role of stereotactic radiosurgery in the management of intracranial tumors. *Oncology* 1990;4:21–31.
155. Dooms GC, Hecht S, Brant-Zawadzki M, Berthiaume Y, Norman D, Newton TH. Brain radiation lesions: MR imaging. *Radiology* 1986;158: 149–155.
156. Wallner KE, Galicich JH, Malkin MG, Arbit E, Krol G, Rosenblum MK. Inability of computed tomography appearance of recurrent malignant astrocytoma to predict survival following reoperation. *J Clin Oncol* 1989; 7:1492–1496.
157. Brooks DJ, Beaney RP, Thomas DGT. The role of positron emission tomography in the study of cerebral tumors. *Semin Oncol* 1986;3:83–93.
158. Kaplan WD, Takvorian T, Morris JH, Rumbaugh CL, Connolly BT, Atkins HL. Thallium-201 brain tumor imaging: a comparative study with pathological correlation. *J Nucl Med* 1987;28:47–52.
159. Brismar T, Collins VP, Kesselberg M. Thallium-201 uptake relates to membrane potential and potassium permeability in human glioma cells. *Brain Res* 1989;500:30–36.
160. Black KL, Hawkins RA, Kim KT, Becker DP, Lerner C, Marciano D. Use of thallium-201 SPECT to quantitate malignancy grade of gliomas. *J Neurosurg* 1989;71:342–346.
161. Kim KT, Black KL, Marciano D, et al. Thallium SPECT imaging of brain tumors: Methods and results. *J Nucl Med* 1990;31:965–969.
162. Mountz JM, Stafford-Schuck K, McKeever PE. Thallium-201 tumor/cardiac ratio estimation of residual astrocytoma. *J Neurosurg* 1988;68: 705–709.
163. Schwartz RB, Carvalho PA, Alexander III E, Loeffler JS, Folkerth R, Holman BL. Radiation necrosis vs high-grade recurrent glioma: differentiation by using dual-isotope SPECT with ^{201}Tl and ^{99m}Tc-HMPAO. *AJNR* 1991;12:1187–1192.
164. Matthew RJ, Meyer JS, Francis DJ, Semchuk KM, Mortel K, Claghorn JL. Cerebral blood flow in depression. *Am J Psychiatry* 1980;137: 1449–1450.
165. Rush AJ, Schlesser MA, Stokely EM, Bonte FJ, Altshuler KZ. Cerebral blood flow in depression and mania. *Psychopharm Bull* 1982;18:6–8.
166. Uytdenhoef P, Portelange P, Jacquy J, Charles G, Linkowski P, Mendlewicz J. Regional cerebral blood flow and lateralized hemispheric dysfunction in depression. *Br J Psychiatry* 1983;143:128–132.
167. Gur RE, Skolnick BE, Gur RC, et al. Brain function in psychiatric disorders. II. Regional cerebral blood flow in medicated unipolar depressives. *Arch Gen Psychiatry* 1984;41:695–699.

168. Devous MD Sr, Rush AJ, Schlesser MA, et al. Single-photon tomographic determination of regional cerebral blood flow in psychiatric disorders. *J Nucl Med* 1984;25:P57.
169. Buchsbaum MS, DeLisi LE, Holcomb HH, et al. Antero-posterior gradients in cerebral glucose use in schizophrenia and affective disorders. *Arch Gen Psychiatry* 1984;41:1159–1166.
170. Kuhl DE, Metter EJ, Riege WH. Patterns of cerebral glucose utilization in depression, multiple infarct dementia, and Alzheimer's disease. In: Sokoloff L, ed. *Brain imaging and brain function.* New York, NY: Raven Press; 1985:211–225.
171. Baxter LR, Phelps ME, Mazziotta JC, et al. Cerebral metabolic rates for glucose in mood disorders. *Arch Gen Psychiatry* 1985;42:441–447.
172. Buchsbaum MS, Wu J, DeLisi LE, et al. Frontal cortex and basal ganglia metabolic rates assessed by positron emission tomography with ^{18}F2-deoxyglucose in affective illness. *J Affective Disord* 1986;10:137–152.
173. Post RM, DeLisi LE, Holcomb HH, Uhde TW, Cohen R, Buchsbaum MS. Glucose utilization in the temporal cortex of affectively ill patients: Positron emission tomography. *Biol Psychiatry* 1987;22:545–553.
174. Kishimoto H, Takazu O, Ohno S, et al. ^{11}C-glucose metabolism in manic and depressed patients. *Psychiatry Res* 1987;22:81–88.
175. Baxter LR, Schwartz JM, Phelps ME, et al. Reduction of prefrontal cortex glucose metabolism common to three types of depression. *Arch Gen Psychiatry* 1989;46:243–250.
176. Schlegel S, Aldenhoff JB, Eisner D, Lindner P, Nickel O. Regional cerebral blood flow in depression: Associations with psychopathology. *J Affective Disord* 1989;17:211–218.
177. Silfverskiold P, Risberg J. Regional cerebral blood flow in depression and mania. *Arch Gen Psychiatry* 1989;46:253–259.
178. Cohen RM, Semple WE, Gross M, et al. Evidence for common alterations in cerebral glucose metabolism in major affective disorders and schizophrenia. *Neuropsychopharmacology* 1989;2:241–254.
179. Reisches FM, Hedde JP, Drochner R. Clinical correlates of cerebral blood flow and depression. *Psychiatry Res* 1989;29:323–326.
180. O'Connell RA, Van Heertum RL, Billick SB, et al. Single photon emission computed tomography (SPECT) with ^{123}I IMP in the differential diagnosis of psychiatric disorders. *J Neuropsychiatry* 1989;1:145–153.
181. Sackeim HA, Prohovnik I, Moeller JR, et al. Regional cerebral blood flow in mood disorders. I. Comparison of major depressives and normal controls at rest. *Arch Gen Psychiatry* 1990;47:60–70.
182. Martinot JL, Hardy P, Feline A, et al. Left prefrontal glucose hypometabolism in the depressed state: A confirmation. *Am J Psychiatry* 1990;147: 1313–1317.
183. Delvenne V, Delecluse F, Hubain P, Schoutens A, De Maertelaer V, Mendlewicz J. Regional cerebral blood flow in patients with affective disorders. *Br J Psychiatry* 1990;157:359–365.
184. Silfverskiöld P, Gustafson L, Risberg J, Rosen I. Acute and late effects of electroconvulsive therapy. Clinical outcome, regional cerebral blood and electroencephalogram. *Ann NY Acad Sci* 1986;462:237–249.
185. Prohovnik I, Sackeim HA, Decina P, Malitz S. Acute reductions of regional cerebral blood flow following electroconvulsive therapy. Interactions with modality and time. *Ann NY Acad Sci* 1986;462:249–262.
186. Silfverskiöld P, Rosen I, Risberg J, Gustafson L. Changes in psychiatric symptoms related to EEG and cerebral blood flow following electroconvulsive therapy in depression. *Eur Arch Psychiatry Neurol Sci* 1987;236: 195–201.
187. Guenther W, Moser E, Mueller-Spahn F, von Oefele K, Buell U, Hippius H. Pathological cerebral blood flow during motor function in schizophrenic and endogenous depressed patients. *Biol Psychiatry* 1986;21: 889–899.
188. Devous MD Sr, Gullion C, Granneman B, Rush AJ. Regional cerebral blood flow alterations in unipolar depression [Abstract]. *J Nucl Med* 1991; 32(5):951–952.
189. Baxter LR Jr. PET studies of cerebral function in major depression and obsessive-compulsive disorder: the emerging prefrontal cortex consensus. *Ann Clin Psychiatry* 1991;3:103–109.
190. Baxter LR, Phelps ME, Mazziotta JC, Guze BH, Schwartz JM, Selin CE. Local cerebral glucose metabolic rates in obsessive-compulsive disorder. *Arch Gen Psychiatry* 1987;44:211–228.
191. Baxter LR, Jr, Schwartz JM, Mazziotta JC, et al. Cerebral glucose metabolic rates in nondepressed patients with obsessive-compulsive disorder. *Am J Psychiatry* 1988;145:1560–1563.
192. Nordahl TE, Benkelfat C, Semple WE, Gross M, King AC, Cohen RM. Cerebral glucose metabolic rates in obsessive compulsive disorder. *Neuropsychopharmacology* 1989;2:23–28.
193. Swedo SE, Schapiro MB, Grady CL, et al. Cerebral glucose metabolism in childhood-onset obsessive compulsive disorder. *Arch Gen Psychiatry* 1989;46:518–523.
194. Debus JR, Devous MD Sr, Cain JW, Battaglia J, Ahmed SN, Rush AJ. Dynanic single photon emission computerized tomography in patients with obsessive compulsive disorder. *Biol Psychiatry* 1989;25:9A.
195. Devous MD Sr. Imaging brain function by single-photon emission computed tomography. In: Andreasen N, ed. *Brain imaging: applications in psychiatry.* Washington, DC: American Psychiatric Press; 1988:147–234.
196. Pearlson GD. PET scans in schizophrenia: what have we learned? *Ann Clin Psychiatry* 1991;3:97–101.
197. Weinberger DR, Berman KF. Speculation of the meaning of cerebral metabolic hypofrontality in schizophrenia. *Schizophr Bull* 1988;14: 157–168.
198. Wolkin A, Jaeger J, Brodie JD, et al. Persistence of cerebral metabolic abnormalities in chronic schizophrenia as determined by positron emission tomography. *Am J Psychiatry* 1985;142:564–571.
199. Paulman RG, Devous MD Sr, Gregory RR, et al. Hypofrontality and cognitive impairment in schizophrenia: dynamic single-photon tomography and neuropsychological assessment of schizophrenic brain function. *Biol Psychiatry* 1990;27:377–399.
200. Matthew RJ, Wilson WH, Tant SR, Robinson L, Prakash R. Abnormal resting regional cerebral blood flow patterns and their correlates in schizophrenia. *Arch Gen Psychiatry* 1988;45:542–549.
201. Gur RE, Skolnick BE, Gur RC, et al. Brain function in psychiatric disorders. I: regional cerebral blood flow in medicated schizophrenics. *Arch Gen Psychiatry* 1983;40:1250–1254.
202. Volkow ND, Brodie JD, Wolfe AP, Angrist B, Russell J, Cancro R. Brain metabolism in patients with schizophrenia before and after acute neuroleptic administration. *J Neurol* 1986;49:1199–1202.
203. Gur RE, Resnick SM, Alavi A, et al. Regional brain function in schizophrenia. I: A positron emission tomography study. *Arch Gen Psychiatry* 1987;44:119–125.
204. Alavi A, Hirsch LJ. Studies of central nervous system disorders with single-photon emission computed tomography and positron emission tomography: Evolution over the past two decades. *Semin Nucl Med* 1992; 21:58–81.
205. Andreasen NC. Evaluation of brain imaging techniques in mental illness. *Ann Rev Med* 1988;39:335–345.
206. Bajc M, Medved V, Basic M, Topuzovic N, Babic D. Cerebral perfusion inhomogeneities in schizophrenia demonstrated with single-photon emission computed tomography and Tc-99m-hexamethylpropyleneamine-oxime. *Acta Psychiat Scand* 1989;80:427–433.
207. Devous MD Sr, Raese JD, Herman JH, et al. Regional cerebral blood flow in schizophrenic patients at rest and during Wisconsin Card Sort task. *J Cereb Blood Flow Metab* 1985;5:S201–S203.
208. Geraud G, Arne-Bes MC, Guell A, Bes A. Reversibility of hemodynamic hypofrontality in schizophrenia. *J Cereb Blood Flow Metab* 1987;7: 9–12.
209. Devous MD Sr, Paulman RG, Herman J, Gregory RR, Bonte FJ, Raese JD. Single-photon tomography studies with schizophrenic patients. *J Clin Exp Neuropsychol* 1988;10:321–322.
210. Berman KF, Zec RF, Weinberger DR. Physiological dysfunction of dorsolateral prefrontal cortex in schizophrenia. II: role of neuroleptic treatment, attention and mental effort. *Arch Gen Psychiatry* 1986;43: 127–135.
211. Berman KF. Cortical "stress tests" in schizophrenia: regional cerebral blood flow studies. *Biol Psychiatry* 1987;22:1304–1326.
212. Daniel DG, Weinberger DR, Jones DW, et al. The effect of amphetamine on regional cerebral blood flow during cognitive activation in schizophrenia. *J Neuroscience* 1991;11:1907–1917.
213. DeLisi LE, Buchsbaum MS, Holcomb HH, et al. Increased temporal lobe glucose use in chronic schizophrenic patients. *Biol Psychiatry* 1989;25: 835–851.
214. Cohen RM, Semple WE, Gross M, et al. Evidence for common alterations in cerebral glucose metabolism in major affective disorders and schizophrenia. *Neuropsychopharmacology* 1989;2:241–254.
215. Buchsbaum MS, DeLisi LE, Holcomb HH, et al. Anteroposterior gradients in cerebral glucose use in schizophrenia and affective disorders. *Arch Gen Psychiatry* 1984;41:1159–1166.
216. Farkas T, Wolfe AP, Jaeger J, Brodie JD, Christman DR, Fowler JS. Regional brain glucose metabolism in chronic schizophrenia: a positron emission transaxial tomographic study. *Arch Gen Psychiatry* 1984;41: 293–300.
217. Buchsbaum MS, Ingvar DH, Kessler R, et al. Cerebral glucography with positron tomography: use in normal subjects and in patients with schiz-

ophrenia. *Arch Gen Psychiatry* 1982;39:251–259.
218. Buchsbaum MS, Wu JC, DeLisi LE, et al. Positron emission tomography studies of basal ganglia and somatosensory cortex neuroleptic drug effects: differences between normal controls and schizophrenic patients. *Biol Psychiatry* 1987;22:479–494.
219. Early TS, Reiman EM, Raichle ME, Spitznagel EL. Left globus pallidus abnormality in never-medicated patients with schizophrenia. *Proc Natl Acad Sci USA* 1987;84:561–563.
220. Resnick SM, Gur RE, Alavi A, Gur RC, Reivich M. Positron emission tomography and subcortical glucose metabolism in schizophrenia. *Psychiatry Res* 1987;24:1–11.
221. Van Heertum RL, O'Connell RA. Functional brain imaging in the evaluation of psychiatric illness. *Semin Nucl Med* 1991;21:24–39.
222. Gur RE, Resnick SM, Gur RC. Laterality and frontality of cerebral blood flow and metabolism in schizophrenia: relationship to symptom specificity. *Psychiatry Res* 1989;27:325–334.
223. Gray BG, Ichise M, Chung D-G, Kirsh JC, Franks W. Technetium-99m-HMPAO SPECT in the evaluation of patients with a remote history of traumatic brain injury: a comparison with x-ray computed tomography. *J Nucl Med* 1992;33:52–58.
224. Reid RH, Gulenchyn KY, Ballinger JR, Venturey RA, ECG. Cerebral perfusion imaging with technetium-99m HMPAO following cerebral trauma: initial experience. *Clin Nucl Med* 1990;15:383–388.
225. Abdel-Dayem HM, Sadek SA, Kouris K, et al. Changes in cerebral perfusion after acute head injury: comparison of CT with Tc-99m HM-PAO SPECT. *Radiology* 1987;165:221–226.
226. Roper SN, Ismael MI, King WA, et al. An analysis of cerebral blood flow in acute closed-head injury using Tc-99m-HMPAO SPECT in computed tomography. *J Nucl Med* 1991;32:684–687.
227. Kung HF, Alavi A, Chang W, et al. In vivo SPECT imaging of CNS D-2 dopamine receptors: initial studies with iodine-123-IBZM in humans. *J Nucl Med* 1990;31:573–579.
228. Schubiger PA, Hasler PH, Beer-Wohlfahrt H, et al. Evaluation of multicentre study with iomazenil: a benzodiazepine receptor ligand. *Nucl Med Commun* 1991;12:569–582.
229. Holman BL, Gibson RE, Hill TC, Eckelman WC, Albert M, Reba RC. Muscarinic acetylcholine receptors in Alzheimer's disease: in vivo imaging with iodine-123-labeled 3-quinuclidinyl-4-iodobenzilate and emission tomography. *JAMA* 1985;254:3063.
230. Weinberger DR, Gibson R, Coppola R, et al. The distribution of cerebral muscarinic acetylcholine receptors in vivo in patients with dementia. A controlled study with ^{123}IQNB and single photon emission computed tomography. *Arch Neurol* 1991;48(2):169–176.
231. Innis RB, Al-Tikriti MS, Zoghbi SS, et al. SPECT imaging of the benzodiazepine receptor: feasibility of in vivo potency measurements from stepwise displacement curves. *J Nucl Med* 1991;32:1754–1761.